Capillary pericytes regulate cerebral blood flow in health and disease

Catherine N. Hall[1*], Clare Reynell[1*], Bodil Gesslein[2*], Nicola B. Hamilton[1*], Anusha Mishra[1*], Brad A. Sutherland[3], Fergus M. O'Farrell[1], Alastair M. Buchan[3], Martin Lauritzen[2] and David Attwell[1]

[*] Equal first author

[1]Department of Neuroscience, Physiology & Pharmacology

University College London, Gower St., London, WC1E 6BT, UK

[2]Department of Neuroscience and Pharmacology, and Center for Healthy Aging,

University of Copenhagen, DK-2200 Copenhagen N, Denmark

[3]Acute Stroke Programme, Radcliffe Department of Medicine,

University of Oxford, Oxford, OX3 9DU, UK

Correspondence to (before publication):

David Attwell (d.attwell@ucl.ac.uk)

Correspondence to (after publication)

David Attwell (d.attwell@ucl.ac.uk) or Martin Lauritzen (mlauritz@sund.ku.dk)

Brain blood flow increases, evoked by neuronal activity, power neural computation and are the basis of BOLD functional imaging. However, it is controversial whether blood flow is controlled solely by arteriole smooth muscle, or also by capillary pericytes. We now demonstrate that neuronal activity and the neurotransmitter glutamate release messengers that hyperpolarise pericytes and dilate capillaries, and that this dilation reflects active pericyte relaxation. Glutamate-evoked dilation is mediated by prostaglandin E_2, but requires nitric oxide release to suppress vasoconstricting 20-HETE synthesis. *In vivo*, when sensory input increases cortical blood flow, capillaries dilate before arterioles and are estimated to produce 84% of the increase of blood flow. In pathology, ischaemia leads to a constriction of capillaries by pericytes. We now show that this is followed by pericyte death in rigor, which may irreversibly constrict capillaries and damage the blood-brain barrier. Pericyte death increases on reperfusion, and is reduced by block of glutamate receptors or Ca^{2+} removal, but not by scavenging reactive oxygen species. These data establish pericytes as major regulators of cerebral blood flow and initiators of BOLD functional imaging signals, and suggest prevention of pericyte constriction and death as a strategy to reduce the long-lasting blood flow decrease which contributes to neuronal death after stroke.

Pericytes are isolated contractile cells on capillaries which may regulate cerebral blood flow[1,2] (as well as stabilising newly-formed capillaries[3], maintaining the blood-brain barrier[4-6], contributing to the "glial scar" in pathology[7], and having stem cell properties[8]). Pericytes can be constricted and dilated by neurotransmitters *in vitro*[1,9], via poorly-understood signalling pathways, and heterogeneity of capillary blood flow might reflect differences in pericyte tone[10-12]. Pericytes can constrict *in vivo*, but it was suggested[2] that they do not relax actively to generate the increase in blood flow evoked by neuronal activity[13]. Similar controversy surrounds the effect of pericytes on blood flow in pathology[14,15]. We have now characterised the responses of pericytes in the neocortex and cerebellum to neuronal activity and ischaemia. Surprisingly, our data demonstrate that pericytes are the first vascular elements to dilate during neuronal activity, making them the initiators of functional imaging

signals. Furthermore, they die readily in ischaemia, which is expected to promote brain damage.

Signalling regulating pericyte dilation

We assessed the signalling systems regulating dilation of molecular layer capillaries in cerebellar slices[1]. Because [O_2] modulates the pathways controlling blood flow[13], we used either 95% or 20% O_2 in the superfusate to produce a supra-normal or a physiological [O_2] in the slice[16,17]. Capillaries were defined as vessels <10 μm in diameter that lack a continuous layer of smooth muscle. Their mean diameter was larger ($p=2.3x10^{-4}$) at the lower O_2 level (5.36±0.30 μm (n=59) in 20% and 4.07±0.14 μm (n=154) in 95% O_2). Pericytes on capillaries can be identified by labelling for NG2 proteoglycan or the growth factor receptor PDGFRβ (Fig. 1a), or employing mice expressing DsRed under control of the NG2 promoter[18] (Fig. 1b, c), and are a different cell class from Iba1-expressing perivascular microglia/macrophages[19] (Fig. 1c). For neocortical capillaries in P21 rats the mean density of pericyte somata was 2.2±0.2 per 100 μm of capillary length (950 μm of capillary were analysed in each of 11 confocal stacks). Pericytes extend processes along and around vessels (Fig. 1a-c) which presumably mediate the fast regulation of capillary diameter described below.

Over a 60 minute period without applying any drugs, capillary diameter was extremely stable (see Fig. 4 below). Applying noradrenaline (2 μM), to mimic its release from the locus coeruleus *in vivo*, produced a sustained constriction mediated by pericytes[1] (Fig. 1d, e), which was not affected by O_2 level (Fig. 1f). Superimposing glutamate (500μM), to mimic glutamate release by active neurons[13], produced a capillary dilation at pericyte locations[1] (Fig. 1d, g; Suppl. Movie 1). When quantified as a percentage of the diameter in the absence of drugs, this dilation was twice as large ($p=0.01$) with 20% O_2 as with 95% O_2 (Fig. 1h), possibly due to less production of vasoconstricting 20-HETE in low [O_2] (see below and Ext. Data Fig. 1). Independent of [O_2], most pericytes (72% in 95% O_2 and 70% in 20% O_2) showed a constriction of more than 5% to noradrenaline, and a dilation of more than 5% to glutamate (63% in 95% O_2 (n=154) and 66% in 20% O_2 (n=59)), and the majority of the

pericytes that constricted to noradrenaline also dilated to glutamate (71% in 95% O_2 and 78% in 20% O_2). Glutamate also dilated some capillaries in the absence of pre-constriction by noradrenaline: in 20% O_2, 29% (7/24) of pericytes dilated by more than 5%, which is less (Chi^2 p=0.005) than the 66% of pericytes that dilated more than 5% after pre-constriction with noradrenaline. In the experiments below, noradrenaline was used to pre-constrict capillaries, to facilitate analysis of the signalling underlying glutamate-evoked dilation.

These experiments do not establish which cells the applied noradrenaline and glutamate act on, which may be neurons, astrocytes or pericytes themselves[13], to release the downstream messengers that ultimately control pericyte tone. We can, however, rule out the possibility that noradrenaline generates 20-HETE to constrict pericytes, because blocking 20-HETE synthesis with 1 μM HET0016 did not affect the constriction evoked by noradrenaline (Ext. Data Fig. 2b, g).

Glutamate releases nitric oxide (NO), a vasodilator, when it activates NMDA receptors[13] and applying an NO donor (DETA-NONOate, 100 μM) evoked capillary dilation (Ext. Data Fig. 2m). Blocking NO synthase with L-N^G-nitroarginine (L-NNA, 100 μM) reduced the glutamate-evoked dilation (Fig. 1i, l; ANOVA p=0.002; L-NNA and other signalling blockers used below did not inhibit the noradrenaline-evoked constriction: Ext. Data Fig. 2). Surprisingly, the dilation was not affected by blocking guanylyl cyclase with ODQ (10μM, ANOVA p=1), so NO does not act by raising the level of cyclic GMP in the pericyte (Fig. 1j, m, Ext. Data Fig. 2e). However, when production of the vasoconstrictor 20-HETE was blocked using HET0016 (1 μM), L-NNA no longer inhibited the glutamate-evoked dilation (Fig. 1k, n, ANOVA on black bars in l and n, p=0.0005), implying that NO promotes dilation by preventing 20-HETE formation. Since a robust dilation occurs with both NO and 20-HETE synthesis blocked (Fig. 1k, n), another messenger must be active. Blocking synthesis of epoxy-derivatives of arachidonic acid with MS-PPOH (10 μM) did not affect the dilation (Ext. Data Fig. 2i, ANOVA p=0.92), but blocking EP_4 receptors for prostaglandin E_2 (with 1 μM L-161,982) greatly reduced it (Fig. 1o, p, ANOVA p=0.001). A similar inhibition

of capillary dilation by blocking EP_4 receptors was seen in neocortical pericytes (Fig. 1q, p=0.004). Applying prostaglandin E_2 itself dilated cerebellar capillaries (Ext. Data Fig. 2n). We therefore identify the messenger that dilates capillaries in response to glutamate as prostaglandin E_2 (or a related species active at EP_4 receptors), but this dilation requires NO release to suppress 20-HETE formation (Ext. Data Fig. 1b).

Patch-clamping showed that glutamate (500 μM) or NMDA (100 μM) produced an outward membrane current (Fig. 2a, b, d) in pericytes at -55 to -75 mV (sometimes preceded by a small inward current: Ext. Data Fig. 3). Similarly, stimulation of the parallel fibres evoked an outward current (Fig. 2c-d, 30±4 pA in 12 cells, sometimes preceded by a smaller inward current: Ext. Data Fig. 3). The stimulation-evoked outward current was inhibited (paired t-test p=0.005) by blocking action potentials with TTX (Fig. 2c, reduced to 15±12% (n=4) of its amplitude without TTX, not significantly different from zero, p=0.28), whereas the NMDA-evoked current was unaffected by TTX (reduced by 12±19% in 5 cells, not significant, p=0.56), consistent with stimulation evoking the outward current by generating action potentials that release glutamate. This outward current is expected to hyperpolarize the cells by ~9 mV (see Methods) and decrease voltage-gated Ca^{2+} entry, causing active relaxation[9] (although other sources of Ca^{2+}, as well as cyclic nucleotide levels, may also regulate contractile tone[9,20]). Consistent with this, parallel fibre stimulation produced a dilation of 14.9±3.1% in 21 capillaries in 20% O_2 (Fig. 2e, f, h; Suppl. Movie 2), which (unlike the constriction evoked by noradrenaline) was blocked by TTX and by blocking EP_4 receptors (Fig. 2g-h).

Since an outward current at negative potentials is not consistent with activation of glutamatergic ionotropic receptors, but is consistent with activation of a K^+ current, these data suggest that endogenous glutamate release leads to the generation of PgE_2, which dilates the capillaries by activating an outward K^+ current in pericytes. PgE_2 has previously been reported to activate an outward K^+ current in aortic smooth muscle[21], and to relax kidney pericytes[22].

Pericytes initiate cerebral blood flow increases *in vivo*

To assess whether pericyte relaxation regulates blood flow *in vivo*, we electrically stimulated the whisker pad (at 3 Hz) and used two-photon imaging of the vasculature (labelled with FITC-dextran) in somatosensory cortex to monitor dilations of penetrating arterioles (entering the cortex from the pial surface) and capillaries, in anaesthetised mice expressing DsRed in pericytes (Fig. 3a). The mean capillary diameter *in vivo*, averaged over all capillaries studied (Table 1) was 4.4±0.1 μm in 633 capillary regions. Pericytes were visualised up to 200 μm deep in the cortex (layer 2/3). Brief whisker pad stimulation (2 sec) evoked vessel dilations that peaked just after the end of the stimulation period (~2.5 sec, Fig. 3b). Longer (15 sec) stimulation produced dilations that initially followed the same time course, then dilated further throughout the stimulation (Fig. 3b, Ext. Data Fig. 4). Most imaging employed 15 sec stimuli, which increased the response magnitude and measurement accuracy. Repeated stimulation gave reproducible responses (Ext. Data Fig. 5a, b). To determine which vessels dilate, we segmented the vasculature by the branching order of the vessels, zero being the penetrating arteriole, one the primary capillary branching off the arteriole, etc. (see Ext. Data Fig. 1, and Table 1 for resting diameters, dilations and numbers of each vessel order). Whisker pad stimulation dilated vessels of all orders (Fig. 3c, Table 1). The fraction of vessels responding (i.e. with a dilation >5%) was similar in penetrating arterioles and in 1st order capillaries, while the frequency of capillary responses decreased with increasing order (Fig. 3c).

To establish where vasodilation is initiated, we imaged different orders of vessel simultaneously. Strikingly, 1st order capillaries usually dilated before penetrating arterioles (Fig. 3d, e; Suppl. Movie 3), with vasodilation onset (assessed as the time to 10% of the maximum dilation) in the capillary being on average 1.38±0.38 sec earlier than for the penetrating arteriole (Fig. 3e, f, $p=0.015$). Further along the vascular tree there was no significant difference in the time to dilation of simultaneously imaged capillaries of adjacent order (Fig. 3f, Ext. Data Fig. 5c). Thus, capillaries dilate before the penetrating arteriole

feeding them. Averaging over all vessels of the same order (not just those imaged simultaneously) showed a similar faster dilation of capillaries than of penetrating arterioles (Fig. 3g), with the time to 10% of the maximum dilation for penetrating arterioles (3.7±0.3 sec) being significantly longer than the values (~2.7 sec) obtained for 1st and 2nd order capillaries (p=0.040 and 0.039 respectively, Fig. 3h, Ext. Data Fig. 5d). As expected, the time course of the blood flow increase in capillaries, assessed from the speed of red blood cell movement with line-scanning[23], increased with a time course similar to that of the capillary dilation (Ext. Data Fig. 5f).

The faster onset of dilation in capillaries compared to arterioles indicates that capillary dilation is not a passive response to a pressure increase produced by arteriole dilation. To assess whether pericytes generate this dilation, we measured the diameter changes of capillaries at locations where DsRed-labelled pericytes were present (either somata or processes, responses did not differ significantly at these locations: Ext. Data Fig. 5e) or where no pericyte was visible. The resting diameter of capillaries was larger where pericyte somata or processes were present (4.62±0.09 μm, n=464) than in pericyte-free zones (3.72±0.08 μm, n=168, Mann-Whitney $p=2.7x10^{-7}$), suggesting that pericytes induce an increase of capillary diameter. Dilations greater than 5% were much more frequent at pericyte locations (Fig. 3i; Chi^2 $p=7.5x10^{-11}$), where the responses also tended to be larger ($p=3.2x10^{-5}$ from Kolmogorov-Smirnov test: Fig. 3j-k). These data reinforce the idea that pericytes actively relax to generate the capillary dilation.

In ischaemia pericytes constrict capillaries and die in rigor

Does pericyte control of capillary diameter also play a role in pathology? Some retinal capillaries are constricted by pericytes in response to ischaemia[1], perhaps because pericyte $[Ca^{2+}]_i$ rises when ion pumping is inhibited by ATP depletion. Cortical capillaries also constrict following middle cerebral artery occlusion[14] (MCAO) *in vivo*. In a clinical setting, reperfusion of thrombus-occluded arteries using tPA can be achieved in 1-6 hours[24,25] but, even when arterial flow is restored, a long-lasting reduction of cerebral blood flow can ensue[26-29]. This may reflect pericyte constriction outlasting ischaemia[14], but it is unclear why

the constriction is so prolonged. We examined the effect of ischaemia on pericyte health using propidium iodide to mark cell death.

Live imaging of cerebral cortical slices exposed to simulated ischaemia (oxygen-glucose deprivation with ATP synthesis by glycolysis and oxidative phosphorylation also blocked with iodoacetate and antimycin) revealed that, within ~15 mins, capillaries in the grey matter constricted at spatially restricted regions near pericytes (Fig. 4a-c). In contrast, the diameter of capillaries not exposed to ischaemic solution was stable over 60 mins (reduced by 3.2±3.0%, not significant, p=0.31, n=13, Fig. 4c). While capillaries not exposed to ischaemia showed little pericyte death even after one hour (as assessed by propidium iodide labelling), ischaemia led to most pericytes on capillaries dying after ~40 mins, usually at locations where the earlier constriction had occurred. All capillaries exposed to ischaemia that we examined showed a consistent response, in which the pericytes first constricted the capillaries, and then died (Fig. 4c). Death of pericytes in rigor, after they have been constricted by a loss of energy supply, will tend to produce a long-lasting increase in the resistance of the capillary bed.

To sample more pericytes than is possible while live imaging the capillary diameter, and examine mechanisms contributing to their death, we acquired confocal stacks of brain slices exposed to simulated ischaemia, which were then fixed and labelled for NG2 and/or isolectin B_4. Ischaemia led to pericytes apposed to capillaries dying rapidly in both the white matter of the cerebellum (Fig. 5a, b) and the grey matter of the cortex (Fig. 5c, d). For pericytes exposed to simulated ischaemia as above, ~90% of pericytes died within an hour (Fig. 5b). This was unaffected by blocking action potentials (with TTX, 1 μM) but was halved by blocking AMPA/kainate receptors (25 μM NBQX) or NMDA receptors (50 μM D-AP5, 50 μM MK-801 and 100 μM 7-chlorokynurenate), implying an excitotoxic contribution to pericyte death. When oxygen-glucose deprivation (OGD) alone was employed (without antimycin and iodoacetate), to allow ATP generation when oxygen and glucose were restored, ~40% of pericytes died after one hour, but OGD-evoked death increased 1.5-fold during 1 hour of reperfusion (Fig. 5c, d). Ionotropic glutamate receptor block or removal of external

Ca^{2+} again significantly reduced the death (Fig. 5d), while blocking NO production had a small protective effect and lowering free radical levels by scavenging $O_2^{\cdot-}$ had no significant effect (Fig. 5d, Ext. Data Fig. 6a). Blocking metabotropic glutamate receptors or 20-HETE production, which might prevent $[Ca^{2+}]_i$ rises, or blocking mitochondrial calcium uptake, also had no effect (Ext. Data Fig. 6b).

Pericytes apposed to capillaries, unlike endothelial cells, also died *in vivo* after 90 min of middle cerebral artery occlusion (MCAO, followed by 22.5 hours recovery: Fig. 5e-f, Ext. Data Fig. 6c). In contrast, a sham operation occluding only the internal carotid artery (which lowered cerebral blood flow less than MCAO: see Methods) produced less pericyte death, and a sham operation with no artery occlusion (which did not affect blood flow: see Methods) induced no more death than was seen in naive untreated animals. Thus, pericyte death is a rapid response of the cerebral vascular bed to ischaemia, both in brain slices and *in vivo*.

Discussion

Understanding what initiates the blood flow increase in response to neuronal activity is crucial for understanding both how information processing is powered and how functional imaging signals are generated[30]. Most neurons are closer to capillaries (~8.4 μm distant, in hippocampus[31]) than to arterioles (70 μm distant[31]), suggesting that neurons might adjust their energy supply by initially signalling to pericytes (Ext. Data Fig. 1a). Our data are consistent with this concept: neuronal activity releases messengers that activate an outward membrane current in pericytes (Fig. 2) and dilates capillaries before arterioles (Fig. 3). Capillary dilation implies that there is a resting tone set by the pericytes, perhaps as a result of noradrenaline release by axons from the locus coeruleus, two thirds of the perivascular terminals of which end near capillaries rather than arterioles[32]. Vascular diameter responses can propagate between adjacent pericytes[1,9], but it is not yet known whether arterioles receive a signal to dilate from pericytes, or from vasoactive messengers which reach arterioles later than they reach pericytes. We have identified the main stimulus to pericyte dilation as being EP_4

receptor activation, by prostaglandin E_2 or a related compound, although NO production is also needed to suppress synthesis of the vasocontrictor 20-HETE (Fig. 1, Ext. Data Fig. 1b). These mechanisms are similar to those controlling arteriole dilation, and may reflect glutamate release activating the production of arachidonic acid and its derivatives in astrocytes or neurons[13].

The more frequent occurrence of capillary dilation at pericyte locations (Fig. 3i-k), and the faster onset of capillary dilation than of arteriole dilation *in vivo* (Fig. 3d-h) suggest that pericytes actively relax to dilate capillaries. A previous failure to observe active capillary dilation[2] may reflect two factors. Firstly, in that study[2], unlike ours, the authors were unable to reproducibly evoke blood flow increases by whisker pad stimulation and so used bicuculline to excite neurons: conceivably this induces seizure-like activity which may generate a non-physiological release of vasoconstricting 20-HETE, as well as of dilating messengers. Secondly, the use of thiopental anaesthetic in that study[2] may have reduced blood flow increases, since the same group reported that the closely related anaesthetic thiobutabarbital suppresses neuronally-evoked blood flow increases by 40% compared to those seen using α-chloralose (the anaesthetic that we use)[33]. In addition, the vessels they define as precapillary arterioles[2] (their Fig. 4h), which did show active dilations, appear to have isolated pericytes on them (rather than continuous smooth muscle) and would be called 1st order capillaries in our nomenclature.

Our data suggest that capillaries have two conceptually separate roles in regulating cerebral blood flow. First, by virtue of their closer location to neurons, they detect neuronal activity earlier than arterioles can, and may pass a hyperpolarizing vasodilatory signal back to arterioles (via gap junctions between pericytes or along endothelial cells)[1,9]. Second, capillary vasodilation itself contributes significantly to increasing blood flow directly. To assess the extent to which capillary dilations increase blood flow, we used data from a recent analysis of the vascular tree in mouse cortex[34] (see Methods). For a mean arteriole dilation of 5.9% during prolonged (15 sec) stimulation (Table 1), a capillary dilation of 6.7% (averaged over all capillary orders, Table 1) and ignoring venule dilation, the steady state blood flow was

predicted to increase by 19%. Omitting the capillary dilation predicted a flow increase of only 3%. Thus, capillary dilation is estimated to generate 100x(19-3)/19 = 84% of the steady state increase in blood flow evoked by neuronal activity, and capillaries dilate ~1 second before penetrating arterioles (Fig. 3f, h). These results imply that BOLD functional imaging signals may largely reflect capillary dilation by pericytes.

For ischaemia, our data support, but significantly modify, the suggestion that pericyte constriction[1,14] may be a cause of the long-lasting decrease of cerebral blood flow that occurs even when a blocked artery is opened up after stroke[26-29]. Whereas it was previously envisaged that constriction of capillaries was by healthy pericytes and could be reversed by suppressing oxidative stress[14], we find that, after ischaemia has constricted them (Fig. 4), pericytes die readily (Fig. 5). This death is mediated in part by glutamate, but is not reduced by free radical scavenging, suggesting that the constriction and death differ at least partly in their causes. Pericyte death in rigor will produce a long-lasting decrease of capillary blood flow[26-29], as well as a breakdown of the blood-brain barrier which is normally maintained by pericytes[4-6]. Both of these will contribute to ongoing neuronal damage, highlighting the potential importance of preventing pericyte death as a therapeutic strategy after stroke, particularly in the penumbra of an affected region. To develop this approach, it will be necessary to develop small molecule inhibitors of pericyte death that could be administered, perhaps with tissue plasminogen activator, soon after a stroke has occurred.

Methods summary

Brain slices were made from rats or NG2-DsRed mice and capillaries were imaged as described previously[1] using bright field imaging. The fluorescence of DsRed-labelled capillary pericytes was used to identify pericytes for patch-clamping. Two photon imaging of FITC-dextran-labelled cortical vessels and DsRed-labelled pericytes *in vivo* was performed in mice as previously described for cerebellum[35]. Full details are in the online Methods.

References

1. Peppiatt, C.M., Howarth, C., Mobbs, P. & Attwell, D. Bidirectional control of CNS capillary diameter by pericytes. *Nature* **443**, 700-704 (2006).

2. Fernández-Klett, F., Offenhauser, N., Dirnagl, U., Priller, J. & Lindauer, U. Pericytes in capillaries are contractile *in vivo*, but arterioles mediate functional hyperemia in the mouse brain. *Proc. Natl. Acad. Sci. U.S.A.* **107**, 22290-22295 (2010).

3. Chan-Ling, T., Page, M.P., Gardiner, T., Baxter, L., Rosinova, E. & Hughes, S. Desmin ensheathment ratio as an indicator of vessel stability: evidence in normal development and in retinopathy of prematurity. *Am. J. Pathol.* **165**, 1301-1313 (2004).

4. Bell, R.D., Winkler, E.A., Sagare, A.P., Singh, I., LaRue, B., Deane, R. & Zlokovic, B.V. Pericytes control key neurovascular functions and neuronal phenotype in the adult brain and during brain aging. *Neuron* **68**, 409-427 (2010).

5. Armulik, A., Genové, G., Mäe, M., Nisancioglu, M.H., Wallgard, E., Niaudet, C., He, L., Norlin, J., Lindblom, P., Strittmatter, K., Johansson, B.R. & Betsholtz. C. Pericytes regulate the blood-brain barrier. *Nature* **468**, 557-561 (2010).

6. Daneman, R., Zhou, L., Kebede, A.A. & Barres, B.A. Pericytes are required for blood-brain barrier integrity during embryogenesis. *Nature* **468**, 562-566 (2010).

7. Göritz, C., Dias, D.O., Tomilin, N., Barbacid, M., Shupliakov, O. & Frisén, J. A pericyte origin of spinal cord scar tissue. *Science* **333**, 238-242 (2011).

8. Dore-Duffy, P., Katychev, A., Wang, X. & Van Buren, E. CNS microvascular pericytes exhibit multipotential stem cell activity. *J. Cereb. Blood Flow Metab.* **26**, 613-624 (2006).

9. Puro D.G. Physiology and pathobiology of the pericyte-containing retinal microvasculature: new developments. *Microcirculation* **14**, 1-10 (2007).

10. Villringer, A., Them, A., Lindauer, U., Einhäupl, K. & Dirnagl, U. Capillary perfusion of the rat brain cortex. An in vivo confocal microscopy study. *Circ Res.* **75**, 55-62 (1994).

11. Schulte, M.L., Wood, J.D. & Hudetz, A.G. Cortical electrical stimulation alters erythrocyte perfusion pattern in the cerebral capillary network of the rat. *Brain Res.* **963**, 81-92 (2003).

12. Jespersen, S.N. & Østergaard, L. The roles of cerebral blood flow, capillary transit time heterogeneity, and oxygen tension in brain oxygenation and metabolism. *J. Cereb. Blood Flow Metab.* **32**, 264-277 (2012).

13. Attwell, D., Buchan, A., Charpak, S., Lauritzen, M., MacVicar, B.A. & Newman, E.A. Glial and neuronal control of blood flow. *Nature* **468**, 232-243 (2010).

14. Yemisci, M., Gursoy-Ozdemir, Y., Vural, A., Can, A., Topalkara, K. & Dalkara, T. Pericyte contraction induced by oxidative-nitrative stress impairs capillary reflow despite successful opening of an occluded cerebral artery. *Nat. Med.* **15**, 1031-1037 (2009).

15. Vates, G.E., Takano, T., Zlokovic, B. & Nedergaard, M. Pericyte constriction after stroke: the jury is still out. *Nat. Med.* **16**, 959 (2010).

16. Hall, C.N., Klein-Flügge, M.C., Howarth, C. & Attwell, D. Oxidative phosphorylation, not glycolysis, powers presynaptic and postsynaptic mechanisms underlying brain information processing. *J. Neurosci.* **32**, 8940-8951 (2012).

17. Hall, C.N. & Attwell, D. Assessing the physiological concentration and targets of nitric oxide in brain tissue. *J. Physiol.* **586**, 3597-3615 (2008).

18. Zhu, X., Bergles, D.E. & Nishiyama, A. NG2 cells generate both oligodendrocytes and gray matter astrocytes. *Development* **135**, 145-157 (2008).

19. Krueger, M. & Bechmann, I. CNS pericytes: concepts, misconceptions, and a way out. *Glia* **58**, 1-10 (2010).

20. Hamilton, N.B., Attwell, D. & Hall, C.N. Pericyte-mediated regulation of capillary diameter: a component of neurovascular coupling in health and disease. *Front. Neuroenergetics* **2**, 5 doi: 10.3389/fnene.2010.00005 (2010).

21. Serebryakov, V., Zakharenko, S., Snetkov, V. & Takeda, K. Effects of prostaglandins E_1 and E_2 on cultured smooth muscle cells and strips of rat aorta. *Prostaglandins* **47**, 353-365 (1994).

22. Crawford, C., Kennedy-Lydon, T., Sprott, C., Desai, T., Sawbridge, L., Munday, J., Unwin, R.J., Wildman, S.S.P. & Peppiatt-Wildman, C.M. An intact kidney slice model to investigate vasa recta properties and function in situ. *Nephron Physiol.* **120**, 17-31 (1994).

23. Kleinfeld, D., Mitra, P.P., Helmchen, F. & Denk, W. Fluctuations and stimulus-induced changes in blood flow observed in individual capillaries in layers 2 through 4 of rat neocortex. *Proc. Natl. Acad. Sci. U.S.A.* **95**, 15741-15746 (1998).

24. Khatri, P. et al. Good clinical outcome after ischemic stroke with successful revascularization is time-dependent. *Neurology* **73**, 1066-1072 (2009).

25. Gupta *et al.* Higher volume endovascular stroke centers have faster times to treatment, higher reperfusion rates and higher rates of good clinical outcomes. *J. Neurointervent. Surg.* **doi**: 10.1136/neurintsurg-2011-010245 (2012).

26. Hauck, E.F., Apostel, S., Hoffmann, J.F., Heimann, A. & Kempski, O. Capillary flow and diameter changes during reperfusion after global cerebral ischemia studied by intravital video microscopy. *J. Cereb. Blood Flow Metab.* **24**, 383-391 (2004).

27. Leffler, C.W., Beasley, D.G. & Busija, D.W. Cerebral ischemia alters cerebral microvascular reactivity in newborn pigs. *Am. J. Physiol.* **257**, H266-271 (1989).

28. Nelson, C.W., Wei, E.P., Povlishock, J.T., Kontos, H.A. & Moskowitz, M.A. Oxygen radicals in cerebral ischemia. *Am. J. Physiol.* **263**, H1356-1362 (1992).

29. Baird, A.E., Donnan, G.A., Austin, M.C., Fitt, G.J., Davis, S.M. & McKay, W.J. Reperfusion after thrombolytic therapy in ischemic stroke measured by single-photon emission computed tomography. *Stroke* **25**, 79-85 (1994).

30. Attwell, D. & Iadecola, C. The neural basis of functional imaging signals. *Trends Neurosci.* **25**, 621-625 (2002).

31. Lovick, T.A., Brown, L.A. & Kay, B.J. Neurovascular relationships in hippocampal slices: physiological and anatomical studies of mechanisms underlying flow-metabolism coupling in intraparenchymal microvessels. *Neuroscience* **92**, 47-60 (1999).

32. Cohen, Z., Molinatti, G. & Hamel, E. Astroglial and vascular interactions of noradrenaline terminals in the rat cerebral cortex. *J. Cereb. Blood Flow Metab*. **17**, 894-904 (1997).

33. Lindauer, U., Villringer, A. & Dirnagl, U. Characterization of CBF response to somatosensory stimulation: model and influence of anesthetics. *Am. J. Physiol.* **264**, H1223-1228 (1993).

34. Blinder, P., Tsai, P.S., Kaufhold, J.P., Knutsen, P.M., Suhl, H. & Kleinfeld, D. The cortical angiome: a 3-D interconnected vascular network with noncolumnar patterns of blood flow. *Nature Neurosci.* **16**, 889-897 (2013).

35. Mathiesen, C., Brazhe, A., Thomsen, K. & Lauritzen, M. Spontaneous calcium waves in Bergmann glia increase with age and hypoxia and may reduce tissue oxygen. *J. Cereb. Blood Flow Metab.* **33**,161-169 (2013).

Acknowledgements

We thank Beverley Clark, Alasdair Gibb, Alex Gourine, Clare Howarth, Renaud Jolivet, Christian Madry, Peter Mobbs, Bill Richardson and Angus Silver for comments on the manuscript. Supported by the Fondation Leducq, European Research Council, Wellcome Trust, UK Medical Research Council, Nordea Foundation via Center for Healthy Aging, the Lundbeck Foundation, NOVO-Nordisk Foundation and Danish Medical Research Council.

Table 1: Properties of vessels of different branching order *in vivo*

	Penetrating arteriole	**Capillaries of different order**				**All capillaries**
Order	**0**	**1**	**2**	**3**	**≥4**	**≥1**
Number of regions (on N vessels)	24 (24)	100 (59)	205 (88)	164 (79)	164 (72)	633 (298)
Number responding >5%	13	52	89	60	56	257
Baseline diameter (μm)	12.4±0.9	5.5±0.2	4.6±0.1	4.1±0.1	3.7±0.1	4.4±0.1
Dilation of all regions (%)	5.9±1.3	7.7±1.0	8.3±0.1	5.4±0.1	5.3±0.1	6.7±0.4
Dilation of responders (%)	10.3±1.3	13.8±1.1	17.9±1.1	13.9±1.1	14.0±1.0	15.3±0.6

Figure Legends

Figure 1. Signalling pathways controlling capillary diameter.

a Capillaries in the molecular layer of rat cerebellum labelled using isolectin B_4, with pericytes (arrow) labelled with antibody to NG2 or PDGFRβ. **b** Cerebellar capillaries in NG2-DsRed mouse showing pericytes labelled with DsRed. **c** Neocortical capillaries in NG2-DsRed mouse, with antibody labelling to Iba1. **d** Rat cerebellar capillary being constricted by 2μM noradrenaline (NA) and dilated by superimposed 500μM glutamate (Glut). Line shows lumen diameter. **e** NA evokes a prolonged constriction (95% O_2; a capillary showing a large constriction is shown for clarity). **f** The diameter reached in NA was not affected by O_2 level (diameters in bar graphs are a percentage of the baseline diameter before any drugs). **g** Superimposing Glut dilates capillaries (20% O_2; a capillary showing a large dilation is shown for clarity). **h** The dilation was larger in low [O_2]. **i** The NOS blocker L-N^G-nitroarginine (L-NNA, 100μM) inhibits the Glut-evoked dilation (20% O_2). **j** The guanylyl cyclase blocker ODQ (10μM) does not have the same effect as L-NNA (20% O_2). **k** Blocking 20-HETE production with HET0016 (1μM) abolishes the inhibitory effect of L-NNA (20% O_2). **l** L-NNA alone reduces Glu-evoked dilations at high and low [O_2] (ANOVA p=0.002; p values on graph are from post hoc t-tests). **m** ODQ does not affect the Glut-evoked dilation. **n** HET0016 abolishes the effect of L-NNA at high and low [O_2]. **o, p** Blocking EP_4 receptors with L161,982 (1μM) inhibits the Glut-evoked dilation (o, 20% O_2) at high and low [O_2] (p). Data in d-o are from rat cerebellar capillaries. **q** EP_4 receptor block abolishes Glut-evoked dilation in rat neocortical capillaries (20% O_2). Effects of drugs on baseline diameter are in Ext. Data Fig. 2.

Figure 2. Pericyte membrane current and capillary dilation in cerebellar slices.

a DsRed labelling shows a patch-clamped pericyte in the molecular layer of mouse cerebellum. Lucifer yellow introduced from patch pipette overlaps with DsRed. **b** Glutamate (Glut, 500 μM) and NMDA (100 μM) evoke an outward current at -55 mV. **c** Stimulation of parallel fibres evokes an outward current (at -74 mV) which is blocked by 1 μM TTX. **d**

Mean amplitude of outward currents evoked by stimulation, glutamate and NMDA (panels b-d are in 95% O_2). **e-f** Parallel fibre stimulation (after preconstriction with noradrenaline, NA, 1 μM) in rat cerebellar slice evokes capillary dilation (20% O_2). Images of capillary in 1 μM noradrenaline before and after stimulation (e) and time course of the vessel diameter (f) at the position indicated in e. **g-h** The constriction produced by NA (g) was unaffected by TTX or block of EP_4 receptors with L161,982, which both abolished the stimulation-evoked dilation (h). P values are from a one way ANOVA with Dunnett's post hoc tests.

Figure 3. Active dilation of capillaries by pericytes *in vivo* in mouse cerebral cortex.

a Confocal stack (90μm thick, maximum intensity projection) of vessels (filled with FITC-dextran) *in vivo* in primary somatosensory cortex of NG2-DsRed mouse, with pericytes showing red fluorescence. Enlargement (single image) shows a penetrating arteriole (0th order) giving rise to a capillary (1st order) which splits into 2nd order branches. **b** Average response of 45 capillary regions to 2 sec and 15 sec whisker pad stimulation. **c** Percentage of vessels of different orders (number studied shown on bars) that showed >5% dilation to whisker pad stimulation. **d** Simultaneous imaging (top, white lines show measurement loci) of penetrating arteriole and 1st order capillary: the capillary dilates 3 sec before the arteriole (bottom: explanation of the smoothing of the data in d, e & g is given in Methods and Ext. Data Fig. 4). **e** Time course of dilation in simultaneously imaged penetrating arterioles (0th order) and 1st order capillaries. **f** Time to 10% of peak dilation for (j-1)th order (or 3rd order for $j \geq 4$) vessel minus that of jth order vessel. Capillaries dilate faster than arterioles. **g** Mean time course of dilations in all responding (>5%) penetrating arterioles and 1st and 2nd order capillaries. Inset expands initial phase of the response. **h** Time to 10% of peak dilation in all 0th, 1st and 2nd order responding vessels. **i** Percentage of capillary locations with pericytes present or absent showing >5% dilations. **j** Cumulative probability of capillary diameter changes of a given size (i.e. including "non-responding" capillaries with <5% responses) in 464 pericyte locations and 168 non-pericyte locations. Diameter changes less than zero

(apparent constrictions) represent random changes in capillary diameter and measurement error. **k** Mean responses for the two distributions in j (p value from Mann-Whitney U test).

Figure 4. In ischaemia, pericytes constrict capillaries and then die in rigor

a Top: images of a capillary in a control rat cortical slice in normal solution. Bottom: images of a capillary exposed to simulated ischaemia (oxygen-glucose deprivation with block of glycolysis and oxidative phosphorylation). Right panels show propidium iodide labelling one hour after switching to ischaemic (or continuing normal) solution, with dead pericytes (P) and endothelial cell (EC) indicated. **b** Diameter of vessels in a, at regions indicated, as a function of time. **c** Mean diameter and number of dead pericytes/(100 μm) from 9 capillaries in ischaemia (diameter measured at 18 locations) and 6 capillaries in normal solution (measured at 13 locations). Diameter in ischaemia was significantly reduced compared to control over most of the time course ($p=1.3x10^{-15}$ and $7.7.x10^{-17}$ at 30 and 60 mins). Pericyte death was significantly higher in ischaemia at 40 and 60 mins (Mann-Whitney p=0.041 and 0.021, respectively). With prolonged imaging a few pericytes also died on capillaries in slices not made ischaemic, but this death did not lead to constriction (1.3±1.5 % reduction in diameter at 3 dead pericytes on 2 vessels).

Figure 5. Pericyte death in ischaemia.

a Rat cerebellar white matter capillaries labelled for NG2 and propidium iodide (PI) after 1 hour's superfusion with control solution (white arrow shows living pericyte) or ischaemia solution containing antimycin and iodoacetate (red arrow shows dead pericyte labelled with PI). **b** Percentage of cerebellar pericytes dead in control conditions or after 1 hour's ischaemia (as in a) alone or with action potentials blocked with TTX (1 μM), AMPA/kainate receptors blocked with 25 μM NBQX, or NMDA receptors blocked with 50 μM D-AP5, 50 μM MK-801 and 100 μM 7-chlorokynurenate (p values are from one way ANOVA with Dunnett's post hoc tests). **c** Rat neocortical grey matter capillaries in brain slices labelled for IB_4, NG2 and PI after 1 hour's exposure to control solution or oxygen & glucose deprivation (OGD). **d** Percentage of pericytes (as in c) that were dead after one hour's OGD (No-reoxy) or OGD

followed by 1 hour's superfusion of control solution (Reoxy) with no added drugs, and with iGluR block (NBQX (25 μM), AP5 (50 μM) and 7CK (100 μM)), zero $[Ca^{2+}]_o$ solution, NOS block with 100 μM L-N^G-nitroarginine, or free radical scavenging with 150 μM MnTBAP or 100 μM PBN (pooled data from Ext. Data Fig. 5a). OGD killed pericytes (ANOVA, $p=10^{-13}$) and death increased during reperfusion ($p=3.3x10^{-13}$). iGluR block or zero $[Ca^{2+}]_o$ reduced death (ANOVA with Dunnett's post hoc test, $p=2.7x10^{-4}$ and $6.0x10^{-7}$). Blocking NOS had a small protective effect (p=0.026) while ROS scavenging did not (p = 0.99). **e, f** Confocal images of striatal capillaries labelled with IB_4 and PI (e) and percentage of striatal pericytes and endothelial cells that are dead (f) from the control and treated hemisphere of *in vivo* MCAO (for 90 mins) treated rats (assessed 24 hours after the onset of MCAO), sham-operated rats (with or without the filament being inserted into the internal carotid artery (ICA)), and naïve control animals. More pericytes die than endothelial cells (repeated measures ANOVA; $p=10^{-6}$). For pericytes, but not endothelial cells, cell death is greater in the lesioned hemisphere (main effect of hemisphere, p=0.004; interaction between cell type and hemisphere p=0.003) and cell death is greater in MCAO-lesioned animals than in naïve animals or sham lesioned animals without ICA occlusion (Tukey post hoc tests, p=0.005 and 0.01). See also Ext. Data Fig. 5 for data from cortex.

Methods

Animals

Experiments used Sprague-Dawley or Wistar rats and NG2-DsRed C57BL/6J mice of either sex. Animal procedures were carried out in accordance with the guidelines of the UK Animals (Scientific Procedures) Act 1986, the Danish National Ethics Committee and European Directive 2010/63/EU. Each experiment was conducted on tissue from at least 3 animals on at least 3 different experimental days.

Brain slice preparation.

Slices (200-300 μm thick) were prepared[36] on a vibratome in ice cold oxygenated (95% O_2/5% CO_2) solution. This solution was usually artificial CSF (aCSF) containing (in mM) 124 NaCl, 2.5 KCl, 26 $NaHCO_3$, 1 $MgCl_2$, 1 NaH_2PO_4, 10 glucose, 0.1-1 Na ascorbate, 2 $CaCl_2$ (to which 1 kynurenic acid was added to block glutamate receptors), and slices were incubated at room temperature in the same solution until used in experiments. For Fig. 2e-h, the slicing solution contained (mM) 93 N-methyl-D-glucamine chloride, 2.5 KCl, 30 $NaHCO_3$, 10 $MgCl_2$, 1.2 NaH_2PO_4, 25 glucose, 0.5 $CaCl_2$, 20 HEPES, 5 Na ascorbate, 3 Na pyruvate, 1 kynurenic acid, and the slices were incubated at 34^{o}C in the same solution for 10 mins, and then incubated at room temperature until used in experiments in a similar solution with the NMDG-Cl, $MgCl_2$, $CaCl_2$ and Na ascorbate replaced by (mM) 92 NaCl, 1 $MgCl_2$ 2 $CaCl_2$ and 1 Na ascorbate.

Immunohistochemical labelling of pericytes

Isolectin B_4 binds to α-D-galactose residues in the basement membrane secreted by endothelial cells[37,38], which surrounds pericytes. Cerebellar slices were incubated in FITC-conjugated 10 μg/ml isolectin B_4 (Sigma) for one hour then fixed for 20 mins in 4% PFA, and incubated for 4-6 hrs in 0.05% Triton X-100, 10% goat serum in phosphate-buffered saline at 21°C, then with primary antibody at 21°C overnight with agitation, and then for 4-8 hrs at 21°C with secondary antibody. Primary antibodies were: guinea pig NG2 (from W.B. Stallcup, 1:100), rabbit NG2 (Millipore AB5320, 1:300) and rabbit PDGFRβ (Santa Cruz sc432, 1:200). Secondary antibodies (goat) were: anti-rabbit (Molecular Probes, 1:200) and

anti-guinea pig (Jackson Lab, 1:100). Pericytes, with a bump on a log morphology on capillaries, or located at the junction of capillaries, labelled for NG2 and PDGFRβ (Fig. 1). Since perivascular immune cells are sometimes confused with pericytes[19], we labelled the former with antibody to Iba1 (rabbit Iba1, Synaptic Systems 234003, 1:500) in 7 cortical and 8 cerebellar slices from 5 NG2-DsRed animals, and found that none of 135 (cortex) and 212 (cerebellum) NG2-DsRed labelled perivascular cells co-labelled for Iba1 (although Iba1 labelled 110 cells in the cortical slices and 136 cells in the cerebellar slices, Fig. 1c), implying that pericytes defined by an on-capillary location and NG2 expression differ from perivascular microglia/macrophages.

Imaging capillaries in brain slices

Slices were perfused with bicarbonate-buffered aCSF, as described above, but without the kynurenic acid, at 31-35°C. In experiments using 20% oxygen, the perfusion solution was bicarbonate-buffered aCSF, gassed with 20% O_2, 5% CO_2, and 75% N_2.

For bright-field recording of capillary diameter, sagittal cerebellar slices were prepared from postnatal day 10 (P10)-P21 Sprague-Dawley rats or coronal cortical slices were prepared from P12 rats. On average 1.3 capillary regions were imaged per slice. Capillaries were imaged[1] at ~30 μm depth within the molecular layer of cerebellar slices or the grey matter of somatosensory/motor cortex slices, using a x40 water immersion objective, a Coolsnap HQ2 CCD camera, and ImagePro Plus or Metafluor acquisition software. Images were acquired every 1-5 sec, with an exposure time of 5 msec. Pixel size was 160 or 300 nm. Vessel internal diameters were measured by manually placing a measurement line (perpendicular to the vessel, Fig. 1d) on the image (at locations near visible pericytes which constricted when noradrenaline was applied), using ImagePro Analyzer, Metamorph or ImageJ software, with the measurer blinded as to the timing of drug applications. The end of the measurement line was placed at locations representing the measurer's best estimate of where the rate of change of intensity was greatest across pixels under the vessel edge, and diameter was estimated to a precision of one pixel. Where necessary, images were aligned by manually tracking drift, or by using Image Pro "Align

Global Images" macro. Experiments where changes in focus occurred were excluded from further analysis. Data in the presence of blockers of signalling pathways were compared with interleaved data obtained without the blockers.

For experiments in which the parallel fibres were stimulated in the molecular layer, coronal slices were used to preserve the parallel fibres, and stimuli of 60-100 μs duration, at 50–90 V and 12 Hz, were applied for 25 sec using a patch pipette electrode placed approximately 100 μm away from the imaged vessel. To check that parallel fibres were being successfully activated, the field potential was monitored in the molecular layer using a 4 MΩ patch pipette filled with aCSF. To ensure that pericytes were healthy we excluded capillaries that did not constrict to 1 μM noradrenaline. Stimulation evoked a dilation (Fig. 2e, f) except in 2 capillaries which constricted, presumably due to direct depolarization of a pericyte by the stimulus since when TTX was applied (to one of these vessels) a stimulation-evoked constriction was still seen in TTX: these 2 vessels were excluded from the analysis.

Patch-clamp recordings of pericytes

Coronal slices of cerebellum were prepared[36] from P10-P17 NG2-DsRed C57BL/6J mice. Slices were superfused with bicarbonate-buffered solution containing (mM) 124 NaCl, 26 $NaHCO_3$, 1 NaH_2PO_4, 2.5 KCl, 1 $MgCl_2$, 2.5 $CaCl_2$, 10 glucose, bubbled with 95% O_2/5% CO_2, pH 7.3, at 21-23^oC or 33-36^oC (stimulation evoked currents were not significantly different at the two temperatures and were pooled). Pericytes were identified as DsRed-expressing cells located on capillaries (oligodendrocyte precursor cells also express NG2-DsRed but these can be distinguished from pericytes morphologically and by their position in the parenchyma). Pericytes were whole-cell clamped between -55 and -75 mV with pipettes containing solution comprising (mM) 130 K-gluconate, 4 NaCl, 0.5 $CaCl_2$, 10 HEPES, 10 BAPTA, 2 Na_2ATP, 2 $MgCl_2$, 0.5 Na_2GTP, 0.05 Alexa Fluor 488, pH set to 7.3 with KOH. Electrode junction potentials were compensated. Patch-clamped cells were morphologically confirmed to be pericytes by dye filling. Series resistance was 20-40 MΩ. In 17 cells the mean resting potential was -47.6$\pm$2.1 mV, and the mean input resistance at the resting

potential was 292±27 MΩ. A 30 pA outward current evoked by neuronal activity (see main text) is thus expected to hyperpolarise pericytes by ~9mV.

Imaging of vessels *in vivo*

Animal preparation: 16 adult NG2 DsRed C57BL/6J mice (18-37 g, of either sex) were prepared for experiments by cannulation of the trachea for mechanical ventilation (SAR-830; CWE, Ardmore, PA). Catheters were placed into the left femoral artery and vein and perfused with physiological saline. The end-expiratory CO_2 (microCapstar End-tidal CO_2 Monitor, CWE) and blood pressure (Pressure Monitor BP-1; World Precision Instruments, Sarasota, FL) were monitored continuously in combination with blood gases in arterial blood samples (pO_2 115-130 mm Hg; pCO_2 35-40 mm Hg; pH 7.35-7.45; ABL 700 Series; Radiometer Medical, Brønshøj, Denmark) to ensure the animals were kept under physiological conditions. The temperature was measured and maintained at 37°C during the experiment with a rectal thermometer regulated heating pad (TC-1000 Temperature Controller; CWE). The animals were anaesthetized with xylazine (10 mg/kg i.p.) and ketamine (60 mg/kg i.p.) during surgery, and then switched to alpha-chloralose (50 mg/kg/h i.v.) during the experiment. The skull was glued to a metal plate using cyanoacrylate gel (Loctite Adhesives) and the plate was fixed in the experimental setup. A craniotomy was drilled with a diameter of approximately 4 mm with the center 0.5 mm behind and 3 mm to the right of the bregma over the sensory barrel cortex region. The dura was removed and the preparation covered with 0.75% agarose (type III-A, low EEO; Sigma-Aldrich, St. Louis, MO) and moistened with artificial cerebrospinal fluid (in mM: 120 NaCl, 2.8 KCl, 22 $NaHCO_3$, 1.45 $CaCl_2$, 1 Na_2HPO_4, 0.9 $MgCl_2$ and 2.6 glucose; pH=7.4) at 37°C and bubbled with 95% air/5% CO_2. The craniotomy was covered with a glass coverslip. When experiments were complete, mice were euthanized by intravenous injection of anaesthesia (pentobarbital, 200 mg/ml and lidocaine hydrochloride, 20 mg/ml) followed by decapitation.

Whisker pad stimulation: The mouse sensory barrel cortex was activated by stimulation of the contralateral ramus infraorbitalis of the trigeminal nerve using a set of custom-made

bipolar electrodes inserted percutaneously. The cathode was positioned at the hiatus infraorbitalis (IO), and the anode was inserted into the masticatory muscles[39]. Thalamocortical IO stimulation was performed at an intensity of 1.5 mA (ISO-flex; AMPI, Jerusalem) and lasting 1 ms, in trains of 2 sec or 15 sec at 3 Hz. The stimulation was controlled by a sequencer file running within Spike2 software (version 7.02; Cambridge Electronic Design, England).

Cortical response imaging: For each animal, the haemodynamic response to stimulation was detected using intrinsic optical imaging (IOS) and used to identify the region of brain activated by whisker pad stimulation, for further vascular imaging. Two photon imaging of blood vessels was then conducted near the centre of this activated region. The IOS was recorded on a Leica microscope with 4× magnification that included the entire preparation in the field of view. The light source consisted of LEDs with green light filters and a fast camera (QuantEM 512SC; Photometrics, Tucson) sampled 29 images/sec before and during 15 sec of 3 Hz stimulation. As haemoglobin strongly absorbs green light, the captured light intensity decreases as the total haemoglobin concentration increases during changes in cerebral blood volume and flow[40]. Images during stimulation were subtracted from control images[41], allowing the area of brain where blood flow increases during whisker stimulation to be revealed.

2-photon imaging: 2% w/v fluorescein isothiocyanate-dextran (FITC-dextran, MW 70,000, 50 µl, Sigma-Aldrich) was administered into the femoral vein to label the blood plasma. *In vivo* imaging of blood vessel diameter and pericyte location was performed using a commercial two-photon microscope (SP5, Leica, Wetzlar, Germany), a MaiTai HP Ti:Sapphire laser (Millennia Pro; Spectra Physics, Santa Clara, CA, mean output power 10mW), and a 20× 1.0 N.A. water-immersion objective (Leica). Tissue was excited at 900 nm wavelength, and the emitted light was filtered to collect red and green light from DsRed (pericytes) and FITC-dextran (vessel lumens). Z-stack images were taken to outline the area of interest. XY-time series were taken to image pericytes and blood vessels during stimulation, with a frame size 512 × 300 pixels (170 msec/frame; pixel size was 93-201 nm depending on

the magnification used, with a mean value of 155 nm; pixel dwell time was 1.1 μsec). Image noise was reduced by smoothing images with a maximum intensity 10 frame (1.7 sec) running summation of the green channel showing the FITC-labelled vascular lumen (see Ext. Data Fig. 4a-d for sample images, and the effect this would have on a step increase of diameter and on the dilations shown in Fig. 3d). This channel was then processed to extract blood vessel diameters. Lines were placed across the vessel (perpendicular to the vessel wall) at a spacing of ~20 μm (e.g. Fig. 3d). The edges of the vessel were located using the ImagePro caliper tool, which finds the greatest gradient in light intensity along the line (where d^2intensity/dx^2=0). As for brain slice imaging above, interpolation of the image intensity across pixels allows, in principle, the position of the edge to be estimated to change by less than one pixel, but in practice we measured the diameter with a precision of one pixel. For Fig. 3e and g the time courses of the measured diameter were also smoothed with a 5 point FFT procedure that removes frequencies over 1.16 Hz (OriginLab software), the effect of which is shown in Ext. Data Fig. 4e. Responding capillaries were defined as those showing a change upon stimulation of more than 5% of the initial vessel diameter (since 4.99% was twice the standard deviation of the baseline diameter averaged over all vessels studied). Where multiple regions responded on a single vessel, their response times were averaged for comparison between paired vessels (Fig. 3f and Ext. Data Fig. 5c).

Blood flow in capillaries was assessed from the velocity of red blood cells, which appear as dark patches inside FITC-dextran labelled vessels, using line-scan imaging[23]. Repetitive line-scans (0.358 ms/line of 512 pixels) along the axis of the vessel before, during and after whisker stimulation (3Hz, 15s) were used to form a space-time image in which moving red blood cells produce streaks with a slope that is equal to the inverse of the speed. The slope was calculated using an automated image-processing algorithm[42]. The baseline speed of red blood cells averaged over all capillaries studied was 1.73±0.20 mm/sec (n=49).

Cell death experiments

Chemical ischaemia: For chemical ischaemia experiments (Figs. 4, 5a-b), sagittal cerebellar slices from P21 (Fig. 4) or P7 (Fig. 5a-b) Sprague-Dawley rats were incubated at 37ºC in an

ischaemic solution in which glucose was replaced with 7 mM sucrose and oxygen was removed by equilibrating solutions with 5% CO_2 and 95% N_2. In addition, 2 mM iodoacetate and 25 μM antimycin were added to the ischaemic solution to block ATP generation by glycolysis and oxidative phosphorylation, respectively[43]. Control slices were incubated in aCSF, gassed as usual with 5% CO_2, 95% O_2. Propidium iodide (PI, 37 μM) was added to both solutions to label dead cells. After 60 min incubation in this ischaemic solution, slices were fixed for 20 minutes in 4% paraformaldehyde and immunohistochemistry for NG2 was performed, as described above.

Oxygen-glucose deprivation: For the oxygen-glucose deprivation experiments shown in Fig. 5c-d, coronal forebrain slices were prepared from P21 Sprague Dawley rats then incubated in aCSF in which glucose was replaced with 7 mM sucrose and oxygen was removed by equilibrating solutions with 5% CO_2 and 95% N_2. Control slices were incubated in aCSF, gassed as usual with 5% CO_2, 95% O_2. After 60 min, some slices were immediately fixed in 4% paraformaldehyde, while others were placed in control aCSF, to reoxygenate for a further 60 min. All solutions also contained 37 μM PI and 10 μg/ml FITC-conjugated isolectin B_4 to label dead cells and blood vessels, respectively. Slices were swiftly washed in aCSF prior to fixation for 20 min in 4% paraformaldehyde, washed 3 times in PBS and mounted on microscope slides in Dako hard set mounting medium. Slides were then imaged using a Zeiss LSM 700 or 710 confocal microscope. PI-positive dead vascular and parenchymal cells were counted using ImageJ software, by an experimenter who was blind to their condition. Cells in the 20 μm closest to the slice surface were excluded from analysis to prevent confounds from slicing-induced damage. Dead or alive pericytes were identified by their "bump on a log" morphology on vessels surrounded by isolectin B_4 labelling. To check that pericytes could be identified by isolectin B_4 labelling alone, in parallel experiments we labelled slices for isolectin B_4 and NG2: the great majority (93% of 718 cells assessed) of pericytes identified this way were found to be positive for NG2. Although some pericytes may slightly move away from capillaries after hypoxia or brain injury[44,45], we only counted pericytes apposed to capillaries in this study.

Middle cerebral artery occlusion: Male Wistar rats (Harlan, UK) weighing 253-312g, housed on a 12h light/dark cycle with *ad libitum* access to food and water, underwent transient middle cerebral artery occlusion (MCAO) as previously described[46]. In brief, animals were anaesthetised with 4% isoflurane and maintained in 1.5-2% isoflurane carried in 70% N_2O and 30% O_2. A midline incision was made in the neck, the right external carotid artery was cauterised and cut, and the right common carotid and internal carotid arteries were temporarily ligated. Through a small arteriotomy in the external carotid artery stump, a 4-0 nylon filament coated with silicone at the tip (Doccol, USA) was advanced up the internal carotid artery to occlude the right middle cerebral artery at its origin. For sham animals, the entire procedure was followed except that either: (i) the filament was only advanced up the beginning of the internal carotid artery (ICA) before being withdrawn after 3 mins (sham with ICA occlusion), or (ii) the external carotid artery was permanently ligated (which had no effect on cerebral blood flow) and the common and internal carotid arteries were exposed but not ligated, and the animals remained under anaesthesia for the same length of time as sham animals (sham without ICA occlusion). Core temperature was maintained at 37°C by a rectal thermister probe attached to a heating pad. Cerebral blood flow was continuously monitored by placing a laser Doppler probe (Oxford Optronix, Oxford, UK) over a thinned skull of the MCA territory approximately 4 mm lateral and 1.5 mm caudal to bregma. In MCAO animals, averaged over the period of occlusion, cerebral blood flow on the treated side fell to 34.9$\pm$7.1 % of baseline (n=6) for 90 mins, while in sham animals with ICA occlusion it dropped significantly less to 67.9$\pm$11.0% of baseline (n=3, t-test p=0.035) for 16 mins (this smaller drop occurs because of occlusion of the ICA), and in sham animals without ICA occlusion blood flow was unaffected (104.0±3.9% of baseline, n=3). Following 90 minutes of MCAO, the filament was retracted, and the common carotid artery ligation was released to allow maximal reperfusion. Anaesthesia was then removed, and at 22.5 hours of reperfusion, neurological deficit was assessed by investigating limb symmetry, motor function, activity and sensory stimulation (modified from ref. 47). A maximum score of 15 equates to severe neurological deficit, while a minimum score of 0 implies no neurological deficit. MCAO

animals had a mean score of 7.5±1.7 (n=6), which was significantly greater than that of sham animals with ICA occlusion (0.3±0.3, n=3, p=0.027) and sham animals without ICA occlusion (0±0, n=3 p=0.039, corrected for multiple comparisons). Animals (including an additional 3 naïve control animals) were then anaesthetised, decapitated, and 200 μm forebrain slices were prepared on a vibratome and labelled with PI and FITC-isolectin B_4 in aCSF for 60 min, then washed, fixed, mounted and cortical and striatal images were captured as described above. Live and dead pericytes were counted in both regions as above except that dead endothelial cells were also counted (identified by their elongated nuclei). More pericyte death was seen in brain slices made from naïve control animals in this *in vivo* series of experiments (Fig. 5f) than in experiments studying pericyte death in slices (Fig. 5b, d); this may be because, for the adult rats used for the *in vivo* experiments, it takes longer to kill the animal and remove its brain, than for the younger animals used for slice experiments. The total number of endothelial cells present, and therefore the percentage of dead endothelial cells, was estimated from the total number of pericytes, assuming a 1:3 ratio of pericytes to endothelial cells[48].

Statistics

Data are mean±s.e.m. P values are from ANOVA (univariate, unless otherwise stated) and post-hoc Dunnett's or Student's t-tests, Chi^2 tests, Kolmogorov–Smirnov tests or Mann-Whitney U tests (for non-normally distributed data), as appropriate. Two tailed tests were used. P values quoted in the text are from independent samples t-tests unless otherwise stated. For multiple comparisons, p values are corrected using a procedure equivalent to the Holm-Bonferroni method (for N comparisons, the most significant p value is multiplied by N, the 2nd most significant by N-1, the 3rd most significant by N-2, etc.; corrected p values are significant if they are less than 0.05). Normality of data was assessed using Kolmogorov–Smirnov tests. All statistical analysis was conducted using IBM SPSS21 or Origin statistics software.

Contribution of capillary dilation to cerebral blood flow increases

To assess how capillary dilations increase blood flow in the steady state, we used data from a recent analysis of the vascular tree in mouse cortex[34]. For blood flow from the cortical surface (where for simplicity we assume blood pressure to be constant) through a penetrating arteriole to layer 4 of the cortex, through the array of inter-connected capillaries, and back to the cortical surface through a penetrating venule, that analysis[34] concluded that the resistances (at baseline diameter) of the arteriole, capillary and venule segments of this path were, respectively, 0.1, 0.4 (for a path from an arteriole to a venule separated by ~200 μm, Figs. 5c and 2g of Ref. 34) and 0.2 poise/μm^3, so that capillaries provide 57% of the total resistance. For a mean neuronal activity evoked arteriole dilation of 5.9% during prolonged (15 sec) stimulation (Table 1 of main text), a capillary dilation of 6.7% (averaged over all capillary orders, Table 1) and ignoring venule dilation, then for resistance inversely proportional to the 4th power of diameter (Poiseuille's law) the blood flow should increase by 19% in the steady state. Omitting the capillary dilation predicts a flow increase of only 3%, while omitting the arteriole dilation (so that only capillaries dilate) predicts a flow increase of 15%. Deviations from Poiseuille's law in the capillaries[34] make only a small correction to these values. Thus, capillary dilation is predicted to generate 84% of the steady state increase in blood flow evoked by prolonged neuronal activity. This figure would be reduced somewhat if pial arteriole dilation[49] significantly contributes to the flow increase. For example if pial arterioles are assumed to dilate by the same 5.9% as penetrating arterioles, and to have the same resistance as penetrating arterioles, then the capillary contribution to the blood flow increase is predicted to be 73% (however the larger diameter of pial vessels and their anastomoses[50] suggest that their contribution to the total resistance and blood flow control will be much less than that of the penetrating arterioles).

Methods and Extended Data References

36. Marcaggi, P. & Attwell, D. Endocannabinoid signaling depends on the spatial pattern of synapse activation. *Nature Neurosci.* **8**, 776-781 (2005).

37. Peters, B.P. & Goldstein, I.J. The use of fluorescein-conjugated Bandeiraea simplicifolia B4-isolectin as a histochemical reagent for the detection of alpha-D-galactopyranosyl groups. Their occurrence in basement membranes. *Exp. Cell Res.* **120**, 321-334 (1979).

38. Laitinen,L. Griffonia simplicifolia lectins bind specifically to endothelial cells and some epithelial cells in mouse tissues. *Histochem. J.* **19**, 225-234 (1987).

39. Nielsen, A. & Lauritzen, M. Coupling and uncoupling of activity-dependent increases of neuronal activity and blood flow in rat somatosensory cortex. *J. Physiol.* **533**, 773-785 (2001).

40. Frostig, R.D., Lieke, E.E., Ts'o, D.Y. & Grinvald, A. Cortical functional architecture and local coupling between neuronal activity and the microcirculation revealed by in vivo high-resolution optical imaging of intrinsic signals. *Proc. Natl. Acad.Sci. U.S.A.* **87**, 6082-6086 (1990).

41. Harrison, T.C., Sigler, A. & Murphy, T.H. Simple and cost-effective hardware and software for functional brain mapping using intrinsic optical signal imaging. *J. Neurosci. Methods* **182,** 211-218 (2009).

42. Schaffer, C.B., Friedman, B., Nishimura, N., Schroeder, L.F., Tsai, P.S., Ebner, F.F., Lyden, P.D. & Kleinfeld, D. Two-photon imaging of cortical surface microvessels reveals a robust redistribution in blood flow after vascular occlusion. *PLoS Biol*, **4**, e22 (2006).

43. Allen, N.J., Káradóttir, R. & Attwell, D. A preferential role for glycolysis in preventing the anoxic depolarization of rat hippocampal area CA1 pyramidal cells. *J. Neurosci*. **25**, 848-859 (2005).

44. Dore-Duffy, P.,Owen, C., Balabonov, R., Murphy, S., Beaumont, T. & Rafols, J.A. Pericyte migration from the vascular wall in response to traumatic brain injury. *Microvasc. Res.* **60**, 55-69 (2000).

45. Gonul, E., Duz, B., Kahraman, S., Kayali, H., Kubar, A. & Timurkaynak, E. Early pericyte response to brain hypoxia in cats: an ultrastructural study. *Microvasc. Res.* **64**, 116-119 (2002).

46. Nagel, S., Papadakis, M., Chen, R., Hoyte, L.C., Brooks, K.J., Gallichan, D., Sibson, N.R., Pugh, C. & Buchan, A.M. Neuroprotection by dimethyloxalylglycine following permanent and transient focal cerebral ischemia in rats. *J. Cereb. Blood Flow Metab.* **31**, 132-143 (2011).

47. Garcia, J.H., Wagner, S., Liu, K.F. & Hu, X.J. Neurological deficit and extent of neuronal necrosis attributable to middle cerebral artery occlusion in rats. Statistical validation. *Stroke* **26**, 627-634 (1995).

48. Pardridge, W.M. Blood-brain barrier biology and methodology. J. Neurovirol. **5**, 556-569 (1999).

49. Iadecola, C. Yang, G., Ebner, T.J. & Chen, G. Local and propagated responses evoked by focal synaptic activityin cerebellar cortex. *J. Neurophysiol.* **78**, 651-659 (1997).

50. Blinder, P., Shih,A.Y., Rafie, C. & Kleinfeld, D. Topological basis for the robust distribution of blood to rodent neocortex. *Proc. Natl. Acad. Sci., U.S.A.* **107**, 12670-12675 (2010).

Extended Data Figure Legends

Extended Data Figure 1. Signalling to capillary pericytes in health and disease.

a As vasodilators released from active neurons and their associated astrocytes diffuse through the brain, they encounter pericytes before arteriole smooth muscle because neurons are closer to capillaries than to arterioles[31]. This may partly explain why capillaries dilate before arterioles (main Fig. 3). **b** Oxygen-dependent signalling pathways regulating vessel diameter (after Ref. 13). Neuronal activity leads to the generation of nitric oxide (NO) and arachidonic acid (AA). AA is converted into PgE_2 which dilates vessels via EP_4 receptors, but also into the vasoconstrictor 20-HETE. Production of 20-HETE is inhibited by NO. Together these pathways regulate capillary diameter (main Fig. 1). Larger dilations to glutamate in low [O_2]

may reflect less production of 20-HETE from AA. **c** In ischaemia, the decrease of ATP concentration leads to a rise of $[Ca^{2+}]_i$ in pericytes. This results in some of them contracting and constricting capillaries[1], which will prevent the passage of white and red blood cells. Most pericytes then die (main Figures 4 and 5). Death of pericytes in rigor will produce a long-lasting decrease of cerebral blood flow, and reduce the ability of the microvasculature to increase blood flow in response to neuronal activity.

Extended Data Figure 2. Drug effects on capillary baseline diameter and constriction to noradrenaline.

a Rat capillaries are constricted by 100 μM L-N^G-nitroarginine (L-NNA), suggesting that there is some tonic release of NO in the slice, with a greater constriction occurring at high $[O_2]$ (bars in panels a-d, f-n show percentage of initial drug-free diameter). **b** However, L-NNA does not affect the diameter of vessels preconstricted with noradrenaline (NA; 2 μM, ANOVA p=0.81). **c** The guanylyl cyclase blocker ODQ (10 μM) does not affect baseline capillary diameter, suggesting that the constricting effect of tonic NO release seen in a is not via the cGMP pathway but is via suppression of 20-HETE release. **d** ODQ slightly enhances the constriction achieved with NA (ANOVA p=0.003). P values on the graph are from post hoc t tests. **e** As expected, ODQ blocks cGMP production by guanylyl cyclase, as assessed by radioimmunoassay. **f** Inhibition of 20-HETE formation with 1 μM HET0016 (HET) does not affect baseline capillary diameter (white bars: at 20% O_2, p=0.78; at 95% O_2, p=0.49), presumably because the tonic NO release (in a) is sufficient to suppress tonic 20-HETE release, and there is no significant difference in baseline diameter in the presence of HET between the two O_2 concentrations (t-test p=0.57). Unlike application of L-NNA alone (see a), application of L-NNA and HET together (black bars) does not significantly change capillary diameter (ANOVA compared to HET alone p=0.59). Indeed, comparing vessel diameters in HET + L-NNA with those in L-NNA alone (black bars in f vs. panel a) reveals that HET significantly relieves the constriction produced by L-NNA (ANOVA p=0.03). **g** HET does not affect either the constriction to NA (white bars versus white bars in b, ANOVA, p=0.51) or the diameter of vessels in L-NNA and NA (black bars versus black bars in b, ANOVA

p=0.26). **h, i** MS-PPOH 10μM does not affect the degree of constriction to NA (h, ANOVA p=0.92) or the dilation to glutamate (i; ANOVA p=0.92). **j-l** Blocking EP_4 receptors with 1 μM L161,982 had no effect on baseline diameter in cerebellum (j) or cortex (97.3±1.4% of baseline in 20% O_2, p=0.07, n=34) and also did not affect the constriction to NA in either area (cerebellum: k, ANOVA p=0.90; cortex in 20% O_2: l). **m-n** Applying DETA-NONOate (**m**, 100 μM) or prostaglandin E_2 (**n**, 1 μM) dilated cerebellar capillaries preconstricted with noradrenaline (in 20% O_2).

Extended Data Figure 3. Pericyte current responses in NG2-DsRed mouse cerebellar slices.

Mean initial inward and later outward currents (as in main Fig 2a-d, 95% O_2) evoked in pericytes by stimulation of the parallel fibres, and by superfusion of 500 μM glutamate or 100 μM NMDA. Numbers of cells apply to both black and white bars.

Extended Data Figure 4. Smoothing of the *in vivo* diameter changes.

a Specimen single frame from the image sequence for Fig. 3d. The presence of red blood cells (RBC) leads to apparent holes in the image of the capillary diameter. **b** RBC movement results in the holes being removed when averaging over 10 frames. **c** For a step increase in vessel diameter (top), the effect on the measured diameter time course (bottom) of a running maximum intensity average being calculated over 10 frames starting at each time being considered: the maximum intensity summation results in the largest diameter at any time dominating the smaller diameters at other times, and so the diameter increase is brought forward by 10 frames. If this were not corrected for, the diameter would appear to increase 10 frames (1.72 sec) before it actually does. To correct for this, the time axis needs to be advanced by 1.72 sec. **d** Correction of the 10 frame averaged time courses of the data used for Fig. 3d for the time shift introduced by the averaging. **e** Effect of the 5 point FFT procedure (which removes frequencies over 1.16 Hz) applied to the averaged time courses in d. The smooth dashed lines are the traces plotted in Fig. 3d.

Extended Data Figure 5. Responses of capillaries in somatosensory cortex *in vivo.*

a, b Reproducibility of response to whisker pad stimulation at 101 capillary locations in NG2-DsRed mice. **a** Mean capillary response time courses are the same on repeated stimulation. **b** Responses at 5 and 15 sec into 15 sec whisker pad stimulation did not differ significantly between the 1st and 2nd stimulation. **c** Time to reach a certain percentage of the maximum dilation in (j-1)th order vessel minus that in jth order vessel imaged simultaneously. The time to 10% and 20% of the peak is faster in 1^{st} order capillaries than in 0^{th} order penetrating arterioles (see main text and Fig. 3f), while there are no significant differences between vessels of adjacent orders for any of the other bars shown (t tests: p = 0.33-1; N for each comparison was as in Fig. 3f of the main text). **d** Time course of responses in all responding (>5%) vessels of different order. Arterioles were significantly slower to reach 10% of their peak response than 1^{st} and 2^{nd} order vessels (see main text). **e** The response distributions of capillaries do not differ near pericyte somata or processes (Kolmogorov-Smirnov test, p=0.24; 172 somata locations, 292 process locations). **f** Comparison of time course of dilation of penetrating arterioles and 1st order capillaries with that of the blood flow increase in capillaries (n=49, all orders averaged) assessed by line-scanning (normalised to the average value at the peak from 11.7-13.2 s).

Extended Data Figure 6. Ischaemia-evoked pericyte death in cortical slices and *in vivo*.

a Rat pericyte death is not affected by either of the free radical scavengers MnTBAP (150μM) or PBN (100μM; ANOVA with Dunnett's post hoc test versus no drug control, p=0.78 and p=1, respectively). The amount of pericyte death did not differ between the two different scavengers (ANOVA, p=0.88) so the data from the two scavengers were combined for the analysis in the main text (Fig. 4d). **b** In addition to the drugs discussed in the main text, none of the following drugs affected pericyte death following OGD and reoxygenation (ANOVA with Dunnett's post hoc test versus no drug control): an inhibitor of mitochondrial calcium uptake, Ru360 (50 μM, p=1), the metabotropic glutamate receptor antagonist MCPG (500 μM; p=0.93) or the 20-HETE synthesis blocker HET0016 (HET, 1 μM; p=1). **c** The percentage of dead cerebral cortical pericytes and endothelial cells after 24 hours in the control and treated

hemispheres of MCAO-treated rats, sham-operated animals where a filament was inserted into the ICA but was not advanced far enough to completely occlude the vessel (see Methods), sham animals without ICA occlusion, and naïve animals which did not experience any surgery before being sacrificed. These data were analysed together with the striatal data in the main Fig. 5f. There was no difference in cell death between cortex and striatum (repeated measures ANOVA, p=0.55). A much greater proportion of pericytes died than endothelial cells (repeated measures ANOVA, $p=2.1x10^{-7}$), and pericyte death, but not endothelial cell death, was greater in the lesioned hemisphere (repeated measures ANOVA, effect of hemisphere: p=0.008, interaction between hemisphere and cell type, p=0.007). As expected, most pericyte death occurred in the MCAO treated animals, while sham-operated animals with ICA occlusion showed intermediate levels of death between MCAO and naïve (or sham with no ICA occlusion) animals (Tukey post hoc tests: MCAO vs naïve animals: p=0.004, MCAO vs. sham without ICA occlusion, p=0.01, MCAO vs. sham with ICA occlusion, p=0.20, sham with ICA occlusion vs. naïve, p=0.13).

Supplementary Movies

Suppl. Movie 1

Movie of vessel in Fig. 1d responding to noradrenaline and glutamate in a rat cerebellar slice.

Suppl. Movie 2

Movie of vessel in Fig. 2f responding to noradrenaline and parallel fibre stimulation in a rat cerebellar slice.

Suppl. Movie 3

Movie of penetrating arteriole and primary capillary in Fig. 3e-f, in mouse somatosensory cortex *in vivo*, responding to whisker pad stimulation. The capillary dilates before the arteriole. Green is FITC-dextran; pericytes are labelled with DsRed.

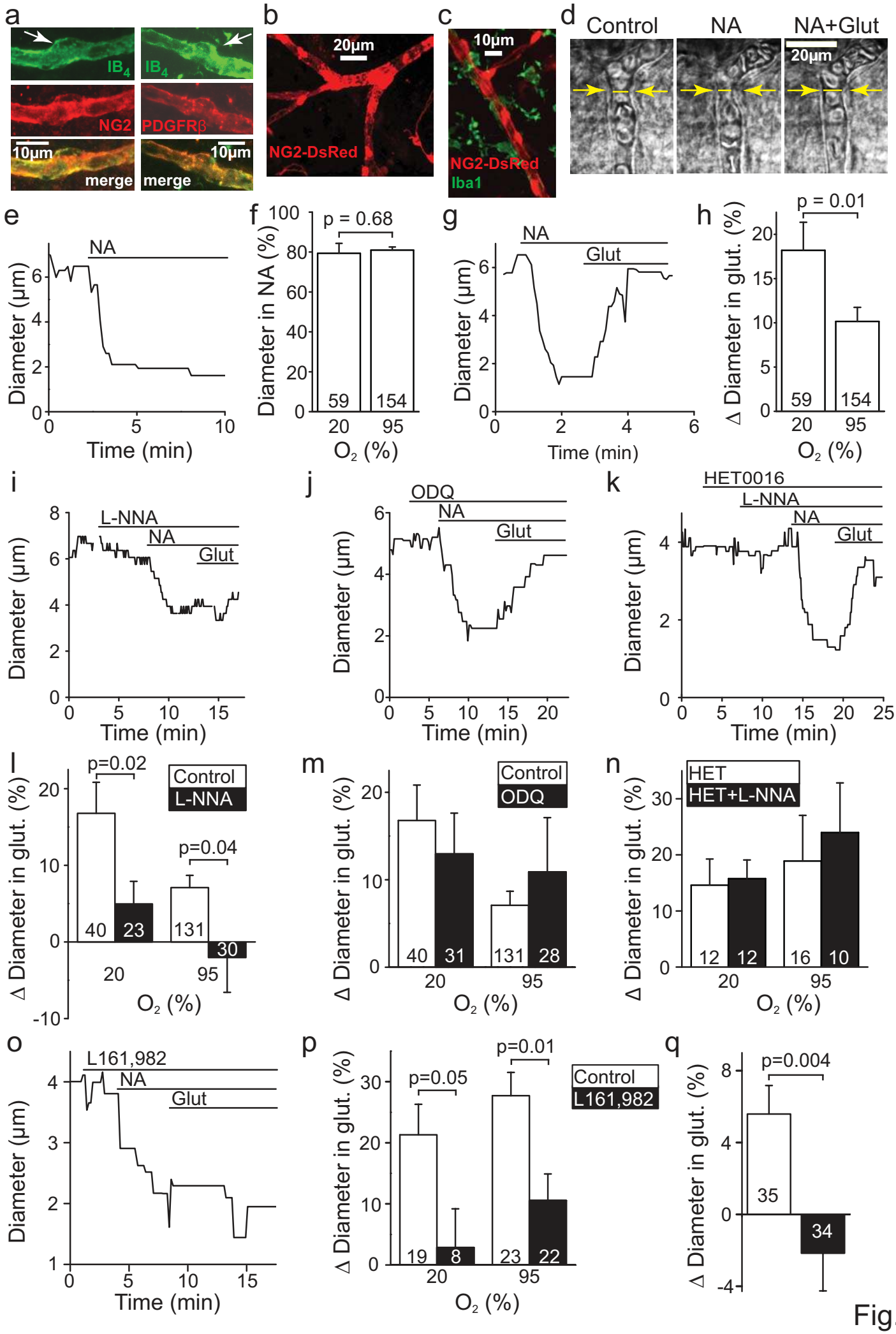
a
IB4
IB4
NG2
PDGFRβ
10μm
merge
10μm
merge
b
20μm
NG2-DsRed
c
10μm
NG2-DsRed
Iba1
d
Control
NA
NA+Glut
20μm
e
NA
Diameter (μm)
Time (min)
f
p = 0.68
Diameter in NA (%)
59
154
20
95
O2 (%)
g
NA
Glut
Diameter (μm)
Time (min)
h
p = 0.01
Δ Diameter in glut. (%)
59
154
20
95
O2 (%)
i
L-NNA
NA
Glut
Diameter (μm)
Time (min)
j
ODQ
NA
Glut
Diameter (μm)
Time (min)
k
HET0016
L-NNA
NA
Glut
Diameter (μm)
Time (min)
l
p=0.02
Control
L-NNA
p=0.04
40
23
131
30
20
95
O2 (%)
Δ Diameter in glut. (%)
m
Control
ODQ
40
31
131
28
20
95
O2 (%)
Δ Diameter in glut. (%)
n
HET
HET+L-NNA
12
12
16
10
20
95
O2 (%)
Δ Diameter in glut. (%)
o
L161,982
NA
Glut
Diameter (μm)
Time (min)
p
p=0.05
p=0.01
Control
L161,982
19
8
23
22
20
95
O2 (%)
Δ Diameter in glut. (%)
q
p=0.004
35
34
Δ Diameter in glut. (%)

Fig. 1

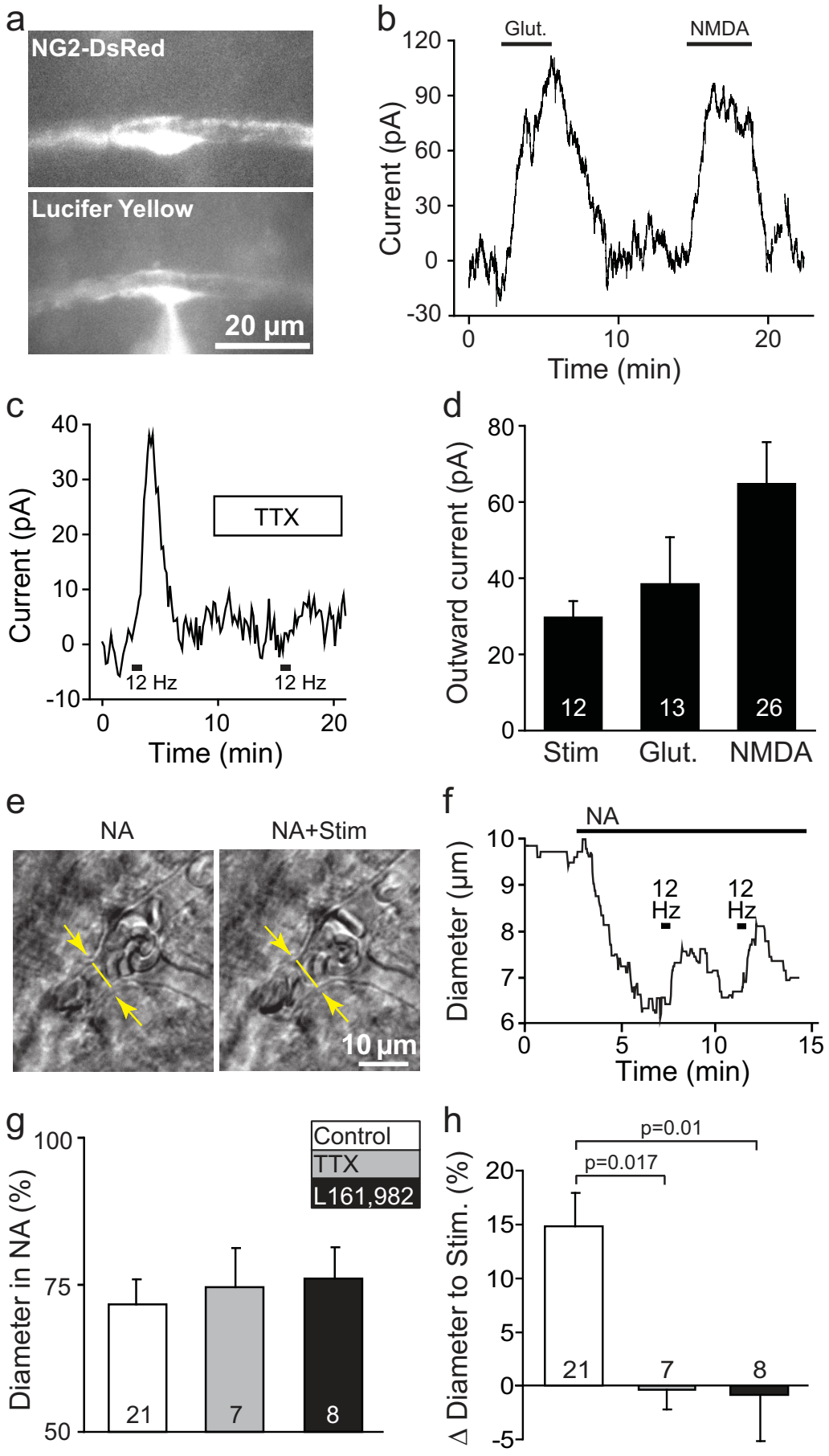
a
NG2-DsRed
Lucifer Yellow
20 µm
b
Glut.
NMDA
Current (pA)
Time (min)
c
TTX
12 Hz
12 Hz
Current (pA)
Time (min)
d
Outward current (pA)
12
13
26
Stim
Glut.
NMDA
e
NA
NA+Stim
10 µm
f
NA
12 Hz
12 Hz
Diameter (µm)
Time (min)
g
Control
TTX
L161,982
Diameter in NA (%)
21
7
8
h
p=0.01
p=0.017
Δ Diameter to Stim. (%)
21
7
8

Fig. 2

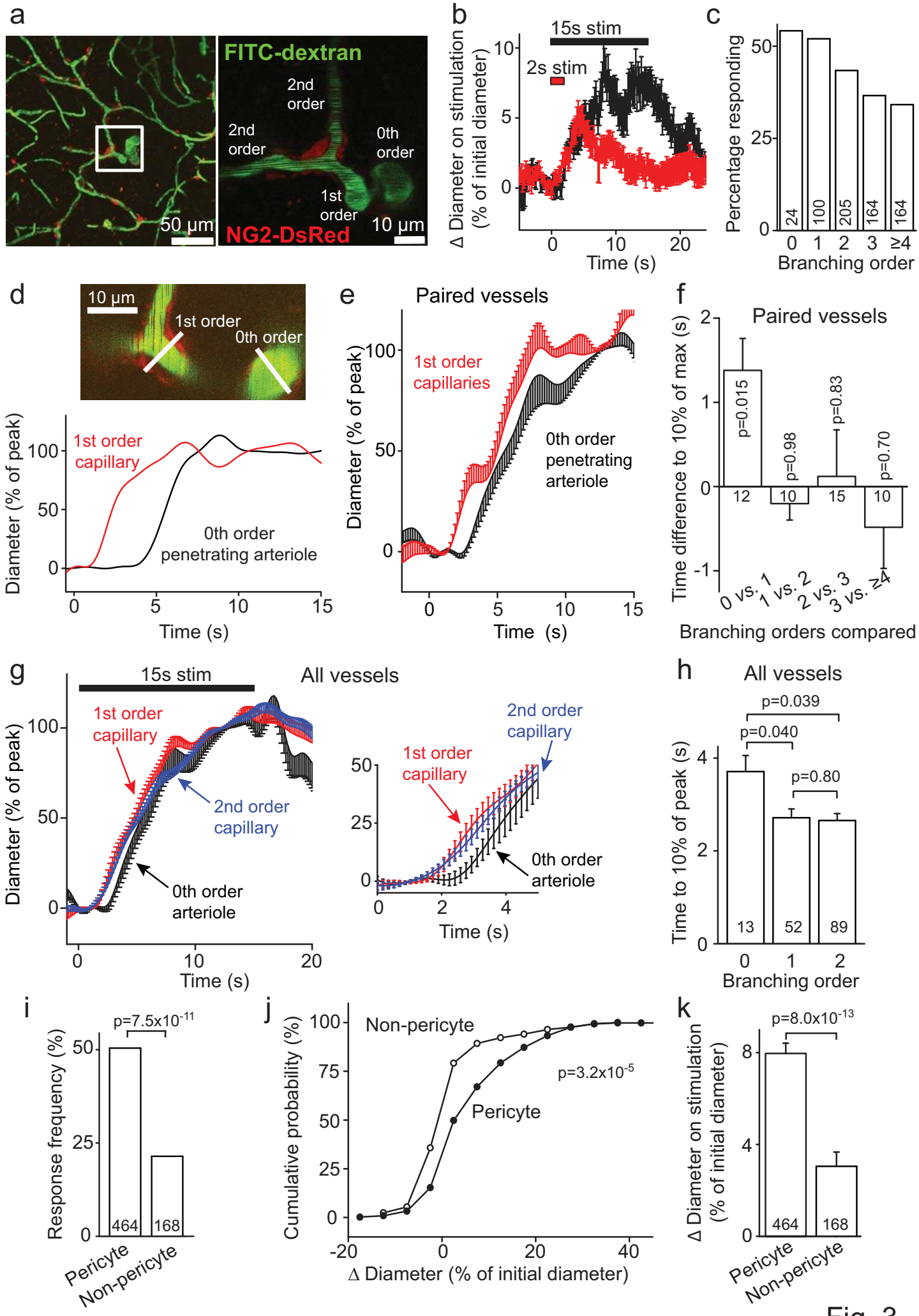
a
FITC-dextran
2nd order
2nd order
0th order
1st order
NG2-DsRed
50 µm
10 µm
b
15s stim
2s stim
Δ Diameter on stimulation (% of initial diameter)
Time (s)
c
Percentage responding
24
100
205
164
164
Branching order
d
10 µm
1st order
0th order
1st order capillary
0th order penetrating arteriole
Diameter (% of peak)
Time (s)
e
Paired vessels
1st order capillaries
0th order penetrating arteriole
Diameter (% of peak)
Time (s)
f
Paired vessels
Time difference to 10% of max (s)
p=0.015
p=0.98
p=0.83
p=0.70
12
10
15
10
0 vs. 1
1 vs. 2
2 vs. 3
3 vs. ≥4
Branching orders compared
g
15s stim
All vessels
1st order capillary
2nd order capillary
0th order arteriole
Diameter (% of peak)
Time (s)
h
All vessels
p=0.039
p=0.040
p=0.80
Time to 10% of peak (s)
13
52
89
Branching order
i
p=7.5x10-11
Response frequency (%)
464
168
Pericyte
Non-pericyte
j
Non-pericyte
p=3.2x10-5
Pericyte
Cumulative probability (%)
Δ Diameter (% of initial diameter)
k
p=8.0x10-13
Δ Diameter on stimulation (% of initial diameter)
464
168
Pericyte
Non-pericyte

Fig. 3

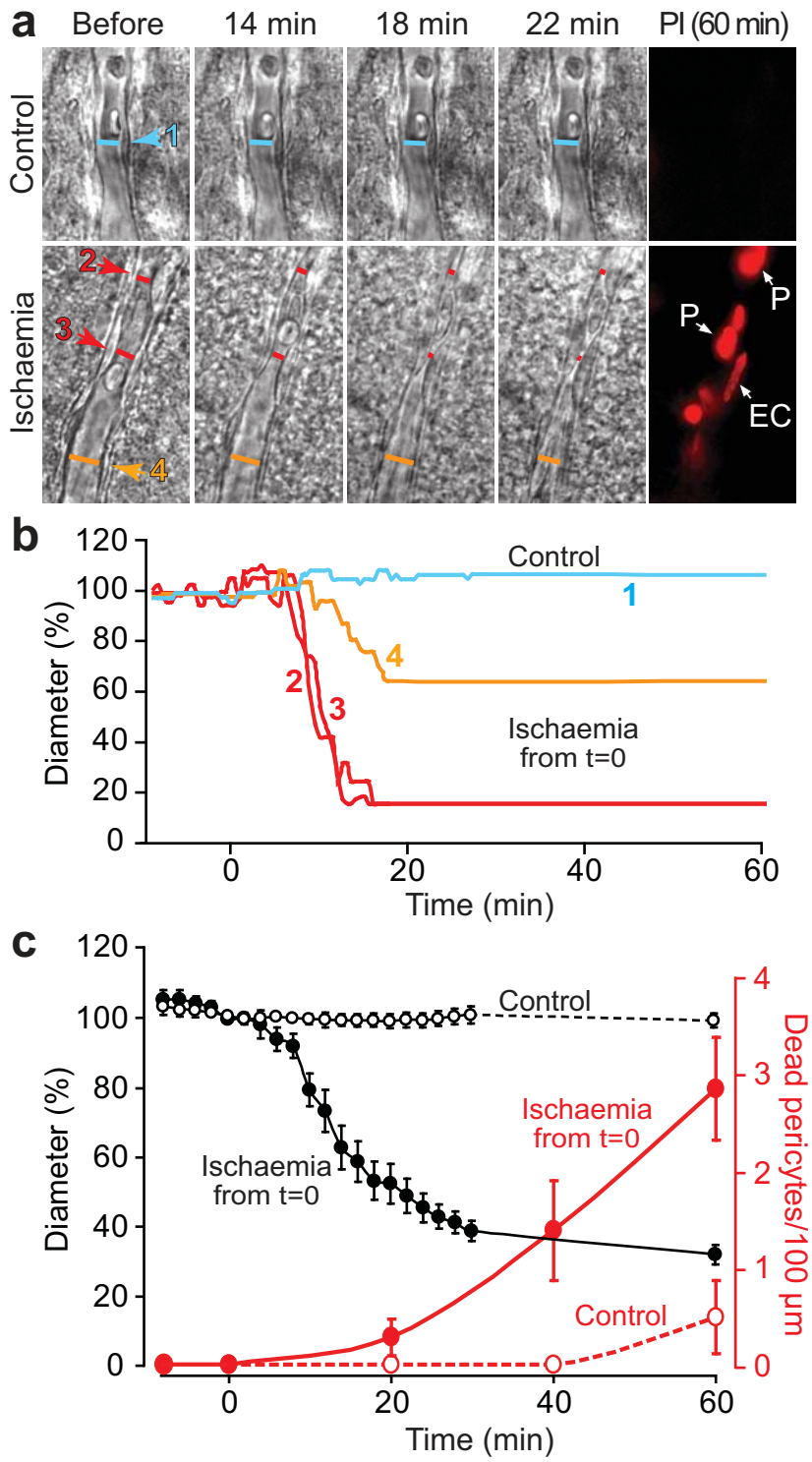
a
Before
14 min
18 min
22 min
PI (60 min)
Control
Ischaemia
1
2
3
4
P
P
EC
b
Diameter (%)
Time (min)
Control
Ischaemia
from t=0
c
Diameter (%)
Dead pericytes/100 µm
Time (min)
Control
Ischaemia
from t=0
Ischaemia
from t=0
Control

Fig. 4

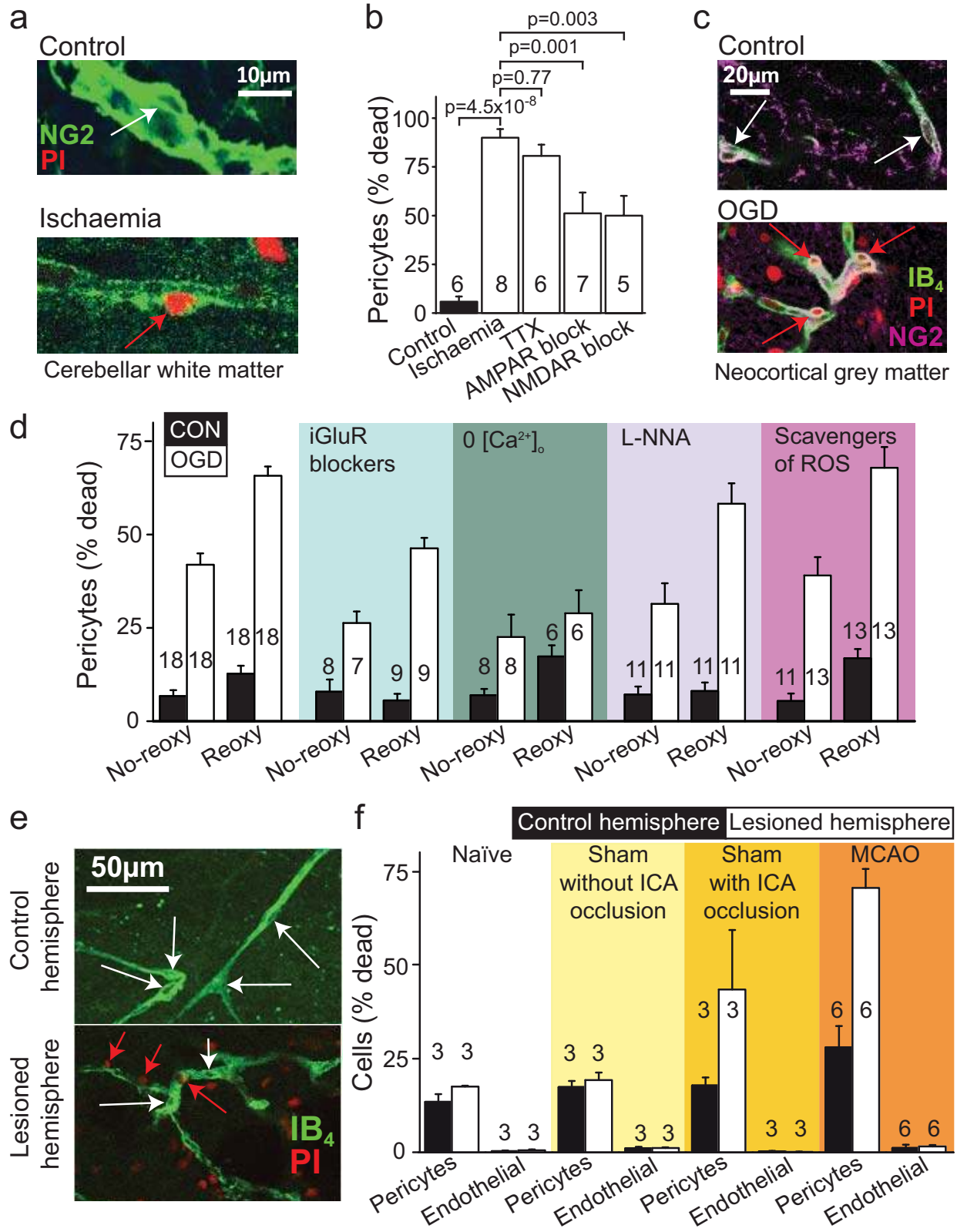
a
Control
10µm
NG2
PI
Ischaemia
Cerebellar white matter
b
p=0.003
p=0.001
p=0.77
p=4.5x10-8
Pericytes (% dead)
100
75
50
25
0
6
8
6
7
5
Control
Ischaemia
TTX
AMPAR block
NMDAR block
c
Control
20µm
OGD
IB4
PI
NG2
Neocortical grey matter
d
CON
OGD
Pericytes (% dead)
75
50
25
0
iGluR blockers
0 [Ca2+]o
L-NNA
Scavengers of ROS
18 18
18 18
8 7
9 9
8 8
6 6
11 11
11 11
11 13
13 13
No-reoxy
Reoxy
e
Control hemisphere
Lesioned hemisphere
50µm
IB4
PI
f
Control hemisphere
Lesioned hemisphere
Cells (% dead)
75
50
25
0
Naïve
Sham without ICA occlusion
Sham with ICA occlusion
MCAO
3 3
3 3
3 3
3 3
3 3
6 6
6 6
Pericytes
Endothelial

Fig. 5

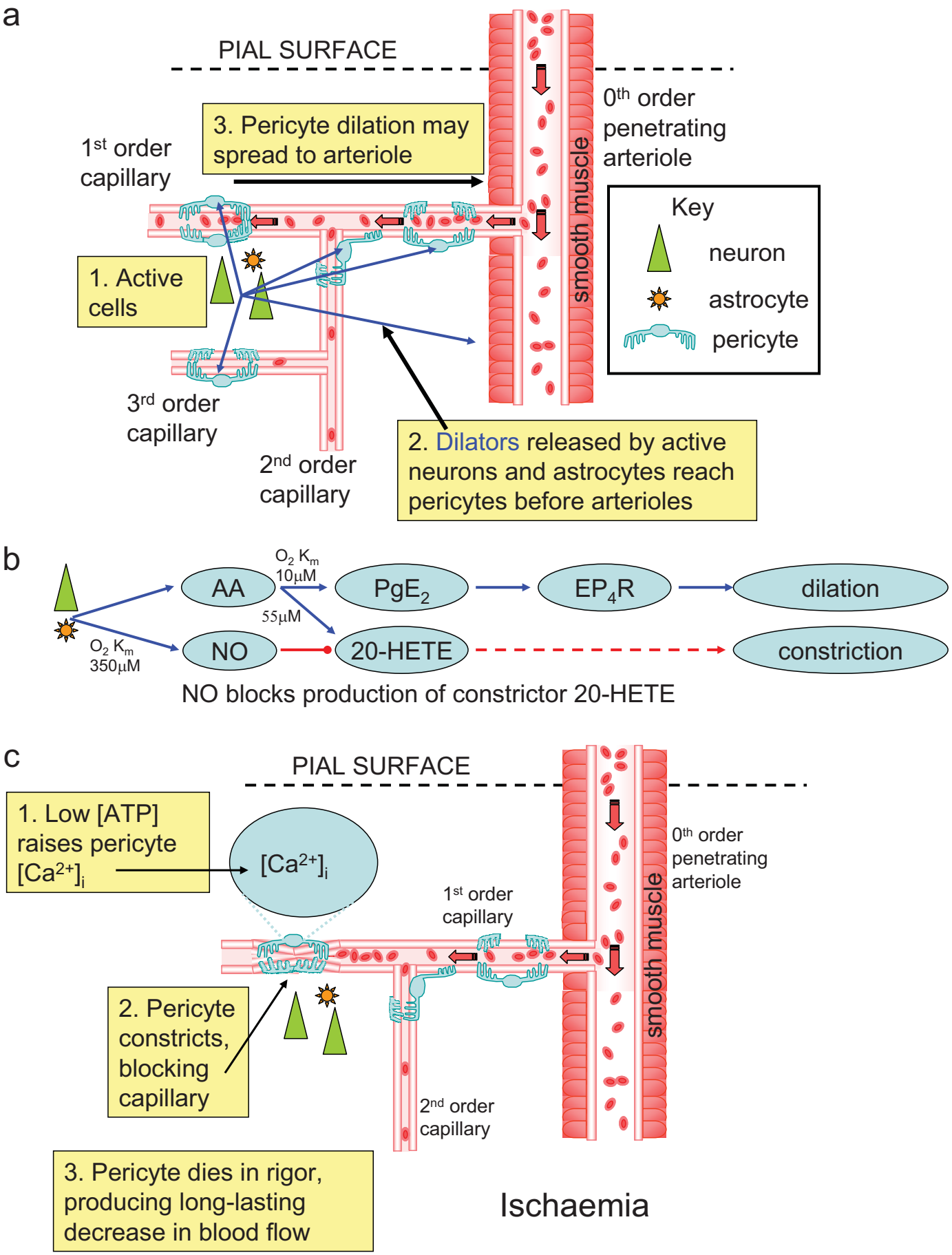

Extended Data Fig. 1

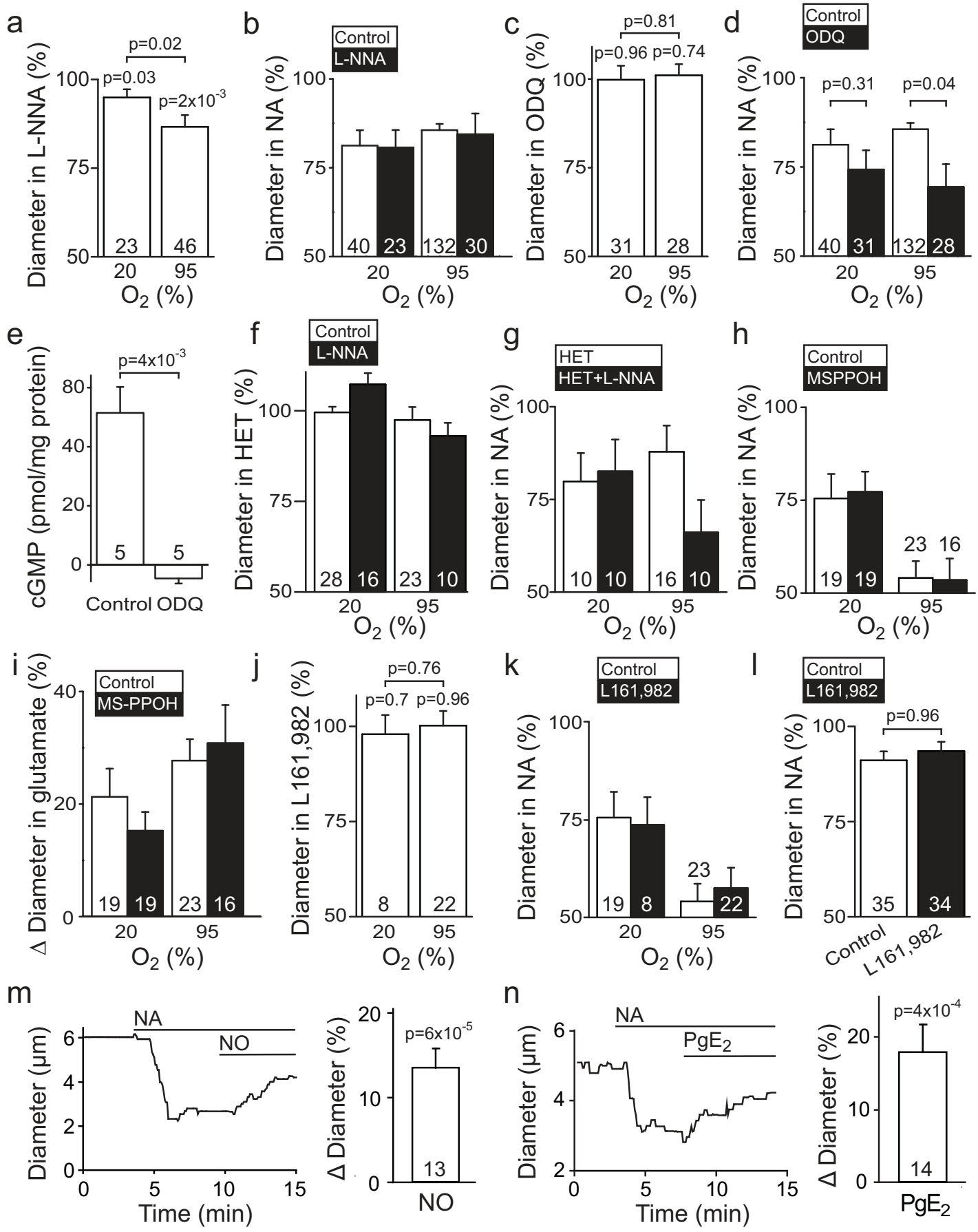

Extended Data Fig. 2

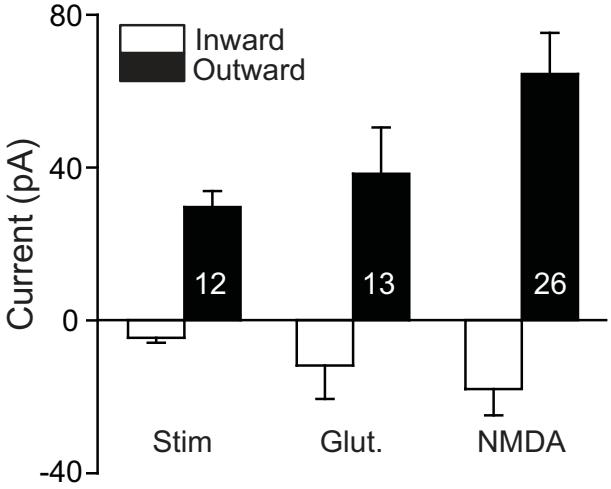

Extended Data Fig. 3

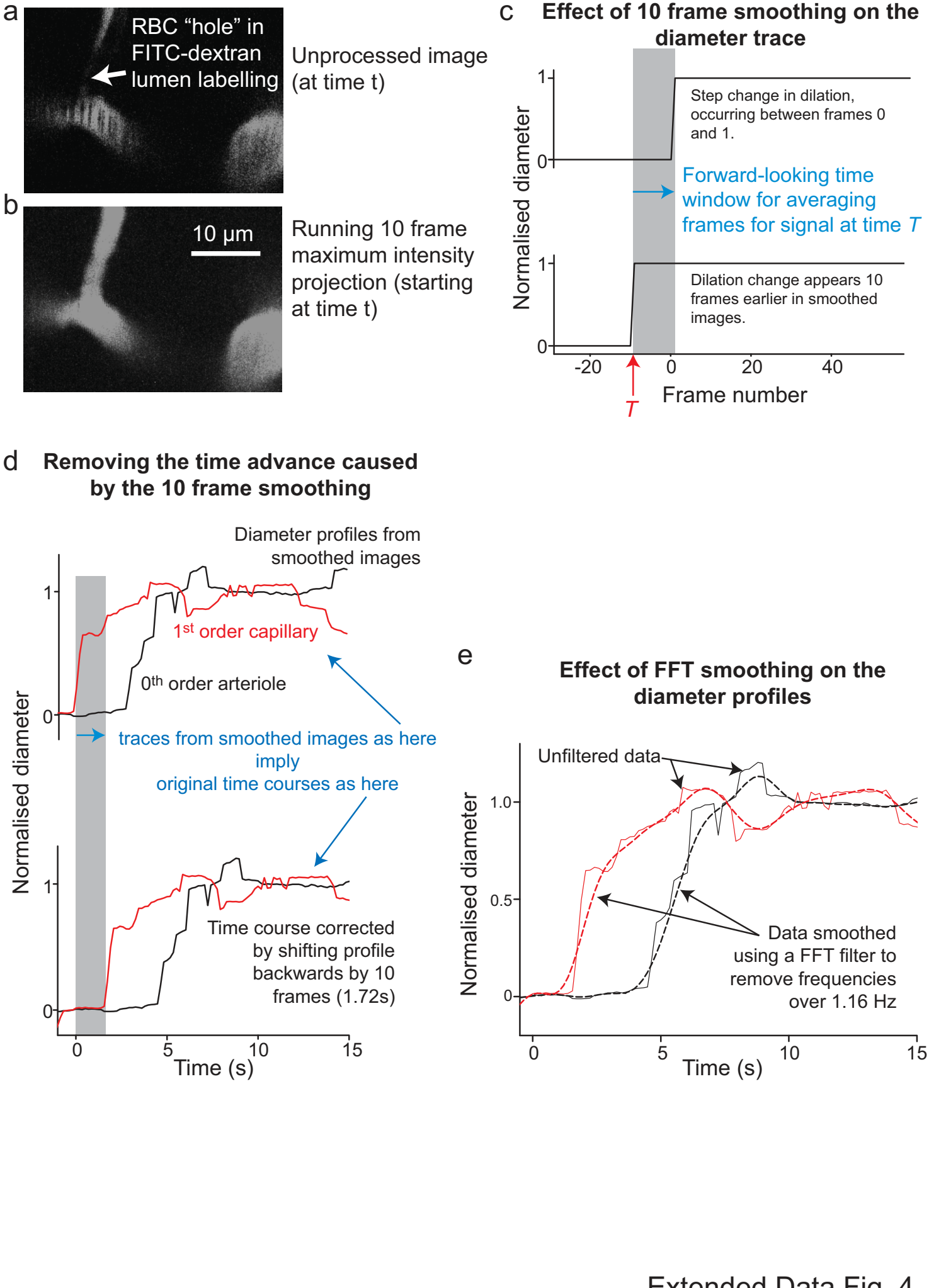

Extended Data Fig. 4

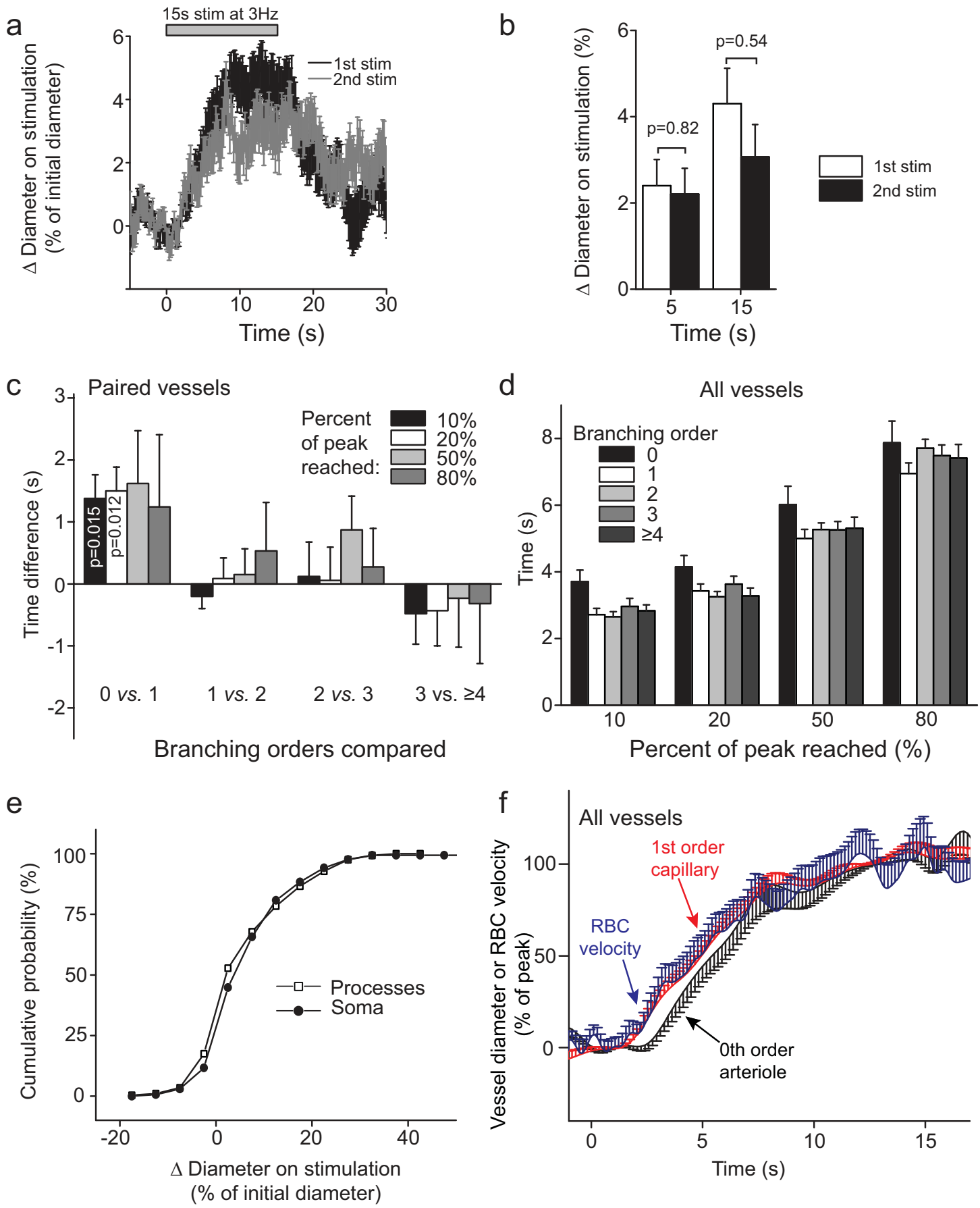

Extended Data Fig. 5

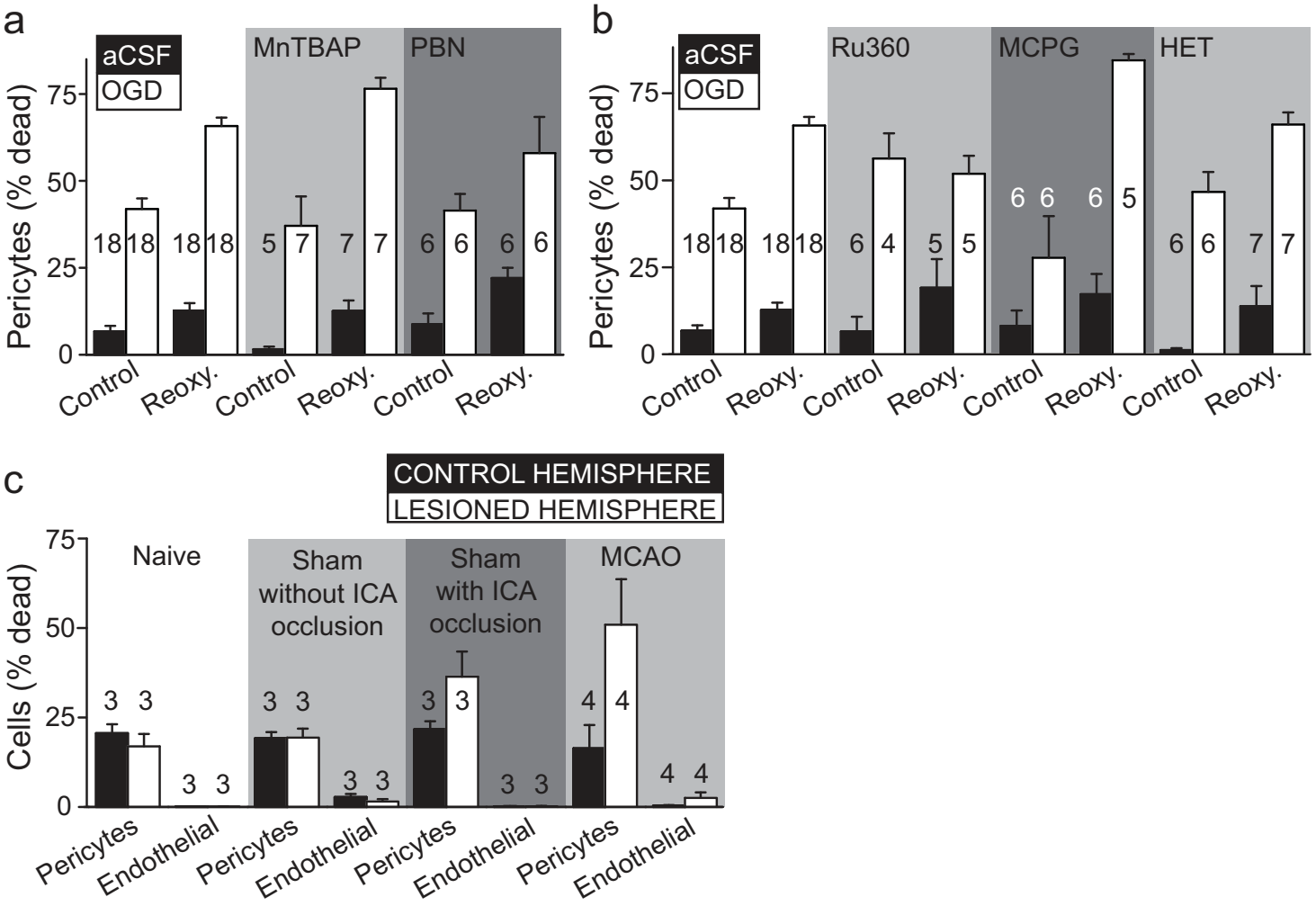

Extended Data Fig. 6